

Development of an Analysis Tool for Impedance data from SiE's Ultra-Thin Cells

Atul Verma

Introduction

A comprehensive model describing physio-chemical processes of the electrode /electrolyte interfaces in the ultrathin SiE cell does not exist at present. Common modeling tool such as Equivalent Circuit Modeling of Electrochemical Impedance Spectroscopy (EIS) data cannot be used as it requires detail knowledge of such physio-chemical processes at each interface in the cell.

A novel computational technique has been developed which does not require *a priori* assumption of an equivalent circuit model to analyze the impedance data. This technique has been used to construct a preliminary equivalent circuit model of SiE cells. Using gas change experiments in the anode and cathode compartments of the cell, the sub circuits associated with each electrode in the equivalent circuit have been identified.

The root cause for the performance degradation behavior of SiE button cells has been investigated using this tool. The anode has been identified as the main component responsible for the observed degradation in the SiE cells. It has been estimated that the high temperature sputter deposited Ni-GDC anodes contribute to ~80% of the overall observed degradation in SiE button cells.

Significance

The solid oxide fuel cell (SOFC) and stack development require an analysis tools for analyzing the impedance data for several projects, such as

1. Cell Degradation Project - The newly developed DRT (Distribution of Relaxation Times) analysis tool is expected to assist in the identification of degrading components. A quantitative assessment of degradation rates of various cell components can be accomplished using this tool.
2. Cell Performance Improvement Project - The new DRT analysis tool is expected to in the identification of key losses associated with the cell components. The improvements in the specific cell components can be measured directly without being smudged by the variation in other cell components during a cell performance improvement project.
3. Cell QC tool development Project –An accurate QC tool which could be used to perform a regular quality checks on the cells and cell components is highly desirable. The newly developed tool could be utilized to directly measure the quality of each cell components in an appropriate unit such as component's area specific resistance.
4. Cell-to-Cell Variability Project– The newly developed tool could be used to measure and assess the performance variation of individual cells and cell-components. The variation in the component resistances could be utilized to assess the cell-to-cell variation within a wafer and between wafers.
5. Root Cause for Cyclic Manufacturing Variability in Cell Production Project - The individual performance of sputtered cathodes, anodes and electrolyte can be

measured as a function of target age, venting schedule and target conditioning. Such direct measurement of cell's individual components is expected to aid the Cyclic Manufacturing Variability Project.

6. SiE Stack Development Project – The DRT analysis could be extended to the impedance measurements on the SiE stacks also. The stack related losses (current collection, fluid flow and thermal effects, etc.) could be identified and measured. A complete assessment of a stack at various operating conditions could be made using the DRT analysis methodology.
7. System Development Project – A complete SOFC system could be characterized using the DRT technique and impact of system operating parameters and fuel processing conditions on the cells and cell components performance can be assessed. Issues such as direct internal reforming (DIR) or in a thermally coupled upstream reformer via the so-called indirect internal reforming (IIR) can be assessed. Similarly, the limits for carbon formation can be explored which happens to be a serious problem with many processes that involve hydrocarbons at high temperatures, including SOFCs. Sulfur compounds, known to act as a catalyst poison, can be monitored.

Background – In recent years, EIS has been established as one of the most important non-destructive characterization methods for electrochemical systems such as fuel cells and batteries. Combined with adequate analysis tools, it has the potential to provide overall understanding of the physical loss processes that form the internal resistance of the electrochemical device under test. Comprehensive details of the technique are described in the textbooks (1-3) and ZVIEW software manual (4).

Electrochemical Impedance Spectroscopy (EIS) - The standard EIS approach is to measure the dynamic behavior (impedance) of an electrochemical system by perturbing the system and measuring phase shift and amplitude of the system response. At very low frequencies (ω_{\min}), all electrochemical loss processes are excited, thus contributing to the measured impedance. The intercept at low frequencies is hence identical with the cell resistance, which can be obtained from the corresponding V_j curve at the given operating point. The measurements at intermediate frequencies, the perturbation signal becomes faster than some of the loss processes and slower loss processes begin to lag the perturbation signal. This results in a phase shift between excitation current and measured voltage response and in a decrease of the response amplitude. Once the excitation signal is much faster than the relaxation frequency of a physical process, the process is not excited anymore. Hence, with increasing ω , an increasing number of physical loss processes do not further contribute to the measured impedance. At very high frequencies, no physical loss processes are excited anymore, resulting in an in-phase voltage response. The high-frequency intercept with the real axis corresponds to the ohmic resistance R_0 of the cell.

Equivalent Circuit Modelling - An equivalent circuit modelling tries to reproduce the impedance response of an electrochemical system based on a hypothesized electrical circuit of a cell. It uses a complex nonlinear least squares (CNLS) fitting algorithm to find a set of parameters. The goodness of the fit is generally evaluated by assessing the relative errors (residuals) between the fit result and the measured curve at each single data point.

The electrochemical devices like fuel cells often exhibit a complex impedance behavior in which several processes contribute to various degree. Small contributions are often overshadowed by large polarization loss processes and deconvolution is often difficult. Another important weakness of the CNLS analysis method is the ambiguity of the equivalent circuits, i.e. various models can be fitted to same data set. Therefore, it is unreliable to assume a model without any knowledge about the real number and physical origin of the polarization processes contributing to the impedance response of the cell.

As such no conclusion about the physical correctness of an equivalent circuit can be drawn from the equivalent circuit modelling alone. The shortcomings of the CNLS-fitting approach can be summarized as follows:

- Poor visual resolution of individual processes in immittance planes,
- A pre-defined/conceived electrical equivalent circuit is required, and
- Ambiguity of the equivalent circuit models.

To overcome these disadvantages an alternative approach for analyzing impedance spectra has been developed. The new approach does not require any assumption of an equivalent circuit but the characteristic relaxation frequency of each polarization process can be precisely determined by the corresponding peak frequency, f_c . The area specific resistance (ASR) as well as degree of dispersion of the underlying physical process can also be measured. With this information, an equivalent circuit model and the optimal starting parameters for the CNLS algorithm can be obtained. The new approach is particularly advantageous for the analysis of cells where the reference electrodes cannot be used for the separation of anode and cathode losses.

A comprehensive model describing physio-chemical processes of the electrode /electrolyte interfaces in the ultrathin SiE can be constructed using this information. However, the ultimate evaluation about the physical correctness of any model should be performed by analyzing the quantitative dependency of the model-parameters for a range of conditions.

Distribution of Relaxation Times

The distribution of relaxation times (DRT) method is since every impedance spectrum can be represented by a sufficiently large number of resistor-capacitor (RC) elements in series [1, 5-14]. For an infinite number of RC elements with continuously increasing relaxation times τ from 0 to ∞ , the impedance $Z(\omega)$ can be expressed by the following integral equation containing the distribution function, $g(\tau)$:

$$Z_{pol}(\omega) = \int_0^{\infty} \frac{g(\tau)}{1 + j\omega\tau} d\tau + R_0 \quad (1)$$

where R_0 reflects the pure ohmic resistance.

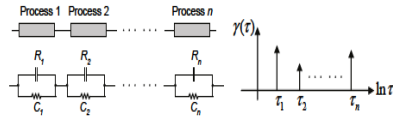
In order to determine the distribution function from the experimentally determined values of Z , one has to solve Eq. 1 for $g(\tau)$.

The solution of $Z_{pol}(\omega)$ using Eq. 1 requires an inversion operation which can be performed using Tikhonov-Regularization technique. A software package called FTIKREG [7] has been used for numerically solving solution the above-mentioned equation. The solution is extremely sensitive to measurement noise in the measured Z . The

distribution function from measured impedance data has been calculated. More detailed information about the DRT can be found in Refs. [5-7].

ECM and DRT Analyses of Impedance Data

Equivalent Ckt Modeling using CNLS (complex Nonlinear Least Square) fittings (using software like EC LAB or ZVIEW)

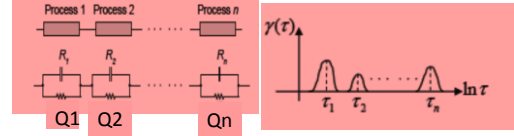


1. Assumes an equivalent ckt with certain number of elements and their arrangements
2. Relies on CNLS fitting with ideal ckt elements (R,C,L W and G) and statistical parameters such as goodness of fit,

$$\chi^2 = \sum \frac{(O - E)^2}{\sigma^2}$$

3. Uses single relaxation time constant, $\tau = 1/RC$ for each process
4. Poor resolution in the frequency domain
5. The equivalent ckts are often unambiguous

Distribution of relaxation times analysis (Ellen Ivers-Tiffée and Bernard Baukamp, Univ of Karlsruhe, Germany)



1. Uses an arbitrary distribution of relaxation times, where each process in the system is represented by a peak,
2. The area under the peak equals the polarization resistance associated with the underlying loss mechanisms.
3. The method relies on the determination of the "distribution function, $g(\tau)$ " from the experimentally determined values of $Z(\omega)$.

$$Z_{pol}(\omega) = \int_0^{\infty} \frac{g(\tau)}{1 + j\omega\tau} d\tau + R_0$$

4. The following inverse problem is solved for $g(\tau)$, $\int_0^b K(\omega, \tau) g(\tau) d\tau = z(\omega)$; called Fredholm Integral Equation of First Kind.
 $K(\omega, \tau)$ is a Kernel function of functions $z(\omega)$ and $g(\tau)$

Fig 1 – Two approaches for the analysis of impedance data - Equivalent Circuit Modeling (ECM) and Distribution of Relaxation Time (DRT)

The benefit of this function is demonstrated in Fig. 2, where the negative imaginary part of the measured impedance spectrum given is compared to the calculated distribution function. Unlike the imaginary part of the complex impedance curve, where the individual polarization processes overlap, four peaks can be distinguished clearly in the DRT. Each peak represents a physical polarization process.

The characteristic relaxation frequency of each polarization process can be precisely determined by the corresponding peak frequency f_c in the DRT. The area enclosed by each peak corresponds to the ASR of the underlying polarization process. Furthermore, peak height $g(f_c)$ and the half-width h_g relative to the peak height give qualitative information about the time-constant dispersion of the underlying physical process.

The high resolution of physical processes in the DRT enables the exact identification of the individual polarization processes that form the impedance spectra of electrochemical devices. Furthermore, impedance analyses by means of the DRT provide (i) a precise determination of the characteristic frequencies of the individual polarization processes as well as (ii) qualitative information about the extent of their contribution to the overall polarization resistance. With this knowledge, a physically meaningful equivalent circuit models can be constructed. The number of passive elements in the equivalent circuit and their peak relaxation frequencies were "estimated" using the FTIKREG program and used as a guide for the CNLS-fit.

The higher resolution of the DRT allows the identification of losses with characteristic peak frequencies clearly distinguished; unlike the impedance curve where

the individual polarization processes overlap, at least five processes be clearly distinguished in the calculated DRT as seen Figure 2.

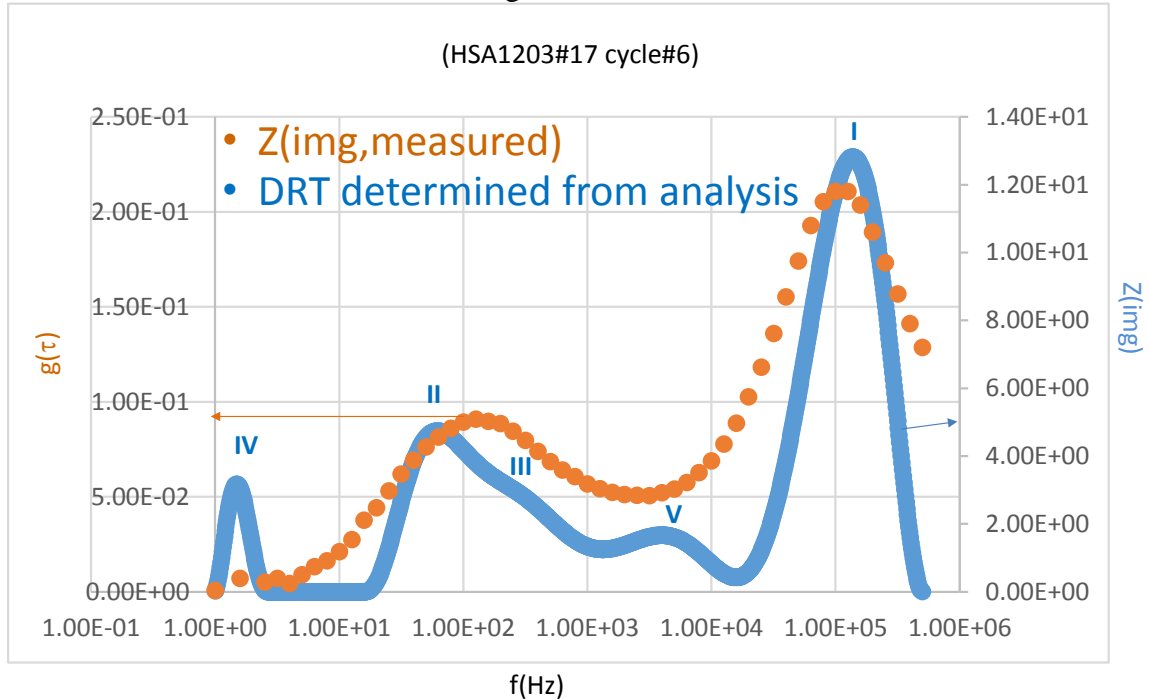


Fig 2 – DRT analysis can deconvolute the cell impedance data and determine that the five (5) independent processes are contributing to the overall cell polarization resistance.

In order to identify peaks associated with contributing polarization processes and investigate their parameter dependency, a series of impedance measurements was carried out in which only one cell parameter at a time was varied (such as cathode oxygen partial pressure or anode hydrogen concentration) (10-14).

In the following sections describe the details of each step of DRT calculation.

1. **FTIKREG program** – A copy of **FTIKREG** (Fast Tikhonov Regularization) program was obtained from Computer Physics Communications Program Library (http://cpc.cs.qub.ac.uk/summaries/ACGH_v1_0.html). The program calculates the functions and distributions which are not accessible experimentally are often related to an experimental accessible quantity by a Fredholm integral equation of the first kind. The solution of the integral equation must be calculated from noisy experimental data, in order to determine such a function or distribution. The description of the solution method and the details of the mathematical foundation is well described in a publication by Wesse [5, 6]. In simple terms, regularization is a process of tuning or selecting the preferred level of model/function complexity so that the models/functions are better at predicting (generalizing). This step makes sure that the final model/function will provides useful predictions, not a too complex function which are achieved by simple least square fitting (overfitting), or too simple model/function caused by under fitting. Basically, apart from fitting,

the complexity parameter (or change the model) is also adjusted to find the value which gives the best model predictions.

2. **Verification of correct operation of the program** – The output provided by program was tested for correctness. The sample data files were also obtained from Computer Physics Communications Program Library (http://cpc.cs.qub.ac.uk/summaries/ACGH_v1_0.html). The samples data files were used to run the program and output files and plots were used to verify the correct operation of the software.
3. **Program modification** - The original FTIKREG program has been written for calculation relaxation distribution from the measurements of viscoelastic properties of polymer which requires minor changes when applied to impedance data. The basic Kernel function needs to be modified when the program is used applied to calculate the distribution of relaxation times from the measured impedances of a SOFC. An editing program (Notepad++, <https://notepad-plus-plus.org/>) for modifying FORTRAN source codes and a FORTRAN compiler - (MinGW, "Minimalist GNU for Windows", <http://www.mingw.org/>), for re-compilation were downloaded and installed.
4. **Program modification for the calculation of distribution of relaxation times from raw impedance data sets** - The Kernel function in the FTIKREG program was modified (FTIKREGv2.f) and the program was re-compiled for the DRT calculations from the imaginary components of the measured impedance data sets. The correct operation of the program was tested with a few synthetic data sets using predetermined equivalent circuits with known time constants. A simple $R_s(RQ)(RQ)$ circuit was constructed and impedance data was synthesized using a commercial software called ZVIEW. The peak frequency of the two (RQ) process was calculated. The DRT analysis was employed using FTIKREG program and the distribution of relaxation times was calculated using the synthetic $Z(\omega)$ data. As shown in the Fig 3 below, the calculated and analyzed peak frequencies, f_{max} matched well which confirms the correct operation of modified routine.

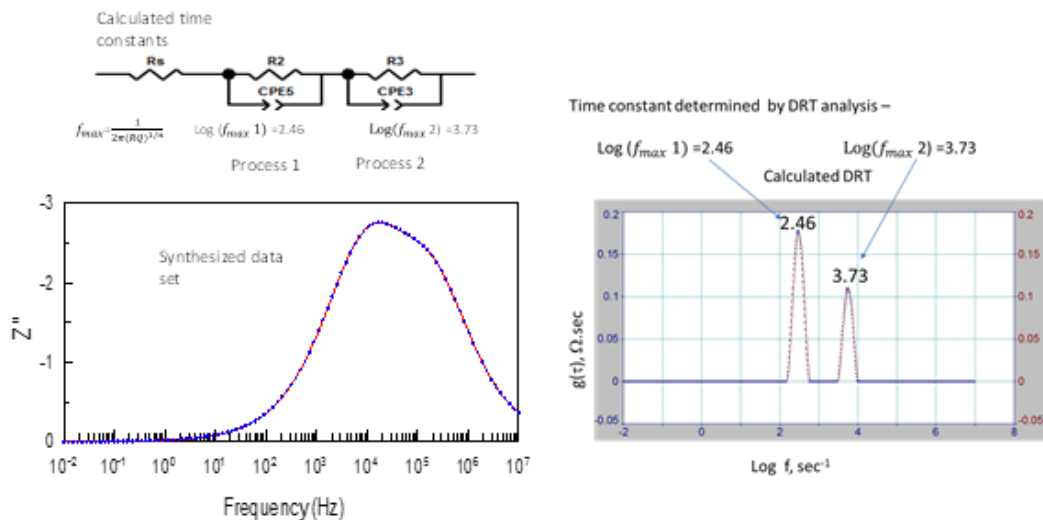


Fig 3 – The correct operation of the modified routine was verified by using synthetic data set. The peak frequencies of the Rs(RQ)(RQ) circuit (left) matched well with the peak frequencies in the DRT analyzed distribution function (right).

5. **Impact of program parameters** - The program FTIKREG reads the parameters from file called FTIKREG.PAR which contains 17 parameter lines. The impact of the program parameters on the outcome was studied by systematically varying these parameters (Fig 4-6). The impact and the results from the study is shown in a table below (Table I).

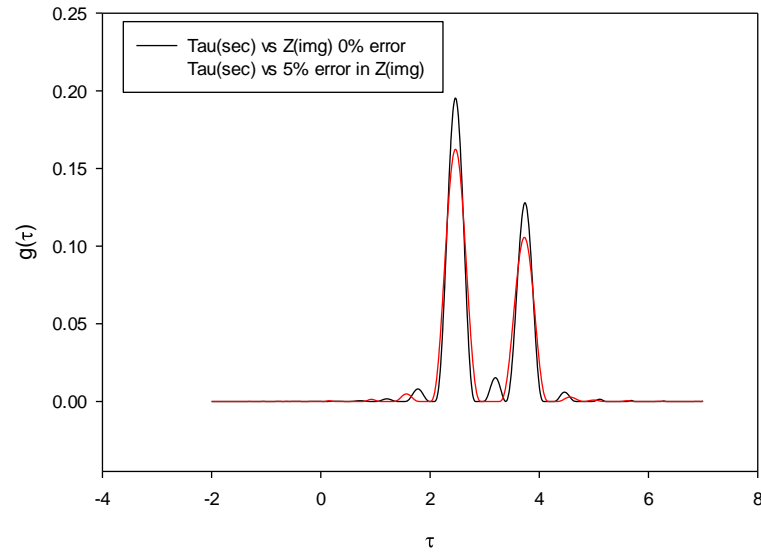


Fig 4 – The DRT analysis with 5% error (uniformly distributed) added shows that the peak position does not change but the oscillations (background noise) increases by adding noise in the impedance data.

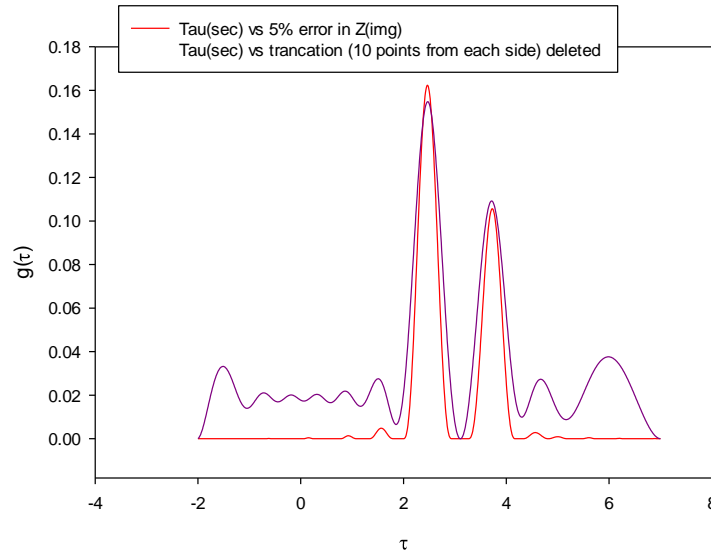


Fig 5 – The DRT analysis with truncated data set shows that the peak position does not change but the oscillations (background noise) increases drastically by truncation.

R _s (X)	R ₂ (X)	CPE5-T(X)	CPE5-P(X)	R ₃ (X)	CPE3-T(X)	CPE3-P(X)
0.5	5	1.00E-05	0.7	8	0.0001	0.65
f _{max} (calculated)		2.22E+05			9.25E+03	
Log f max		5.346149			3.966297	

R _s (X)	R ₂ (X)	CPE5-T(X)	CPE5-P(X)	R ₃ (X)	CPE3-T(X)	CPE3-P(X)
0.5	5	1.00E-05	0.95	8	0.0001	0.95
f _{max} (calculated)		5.36E+03			2.90E+02	
Log f max		3.73E+00			2.46E+00	

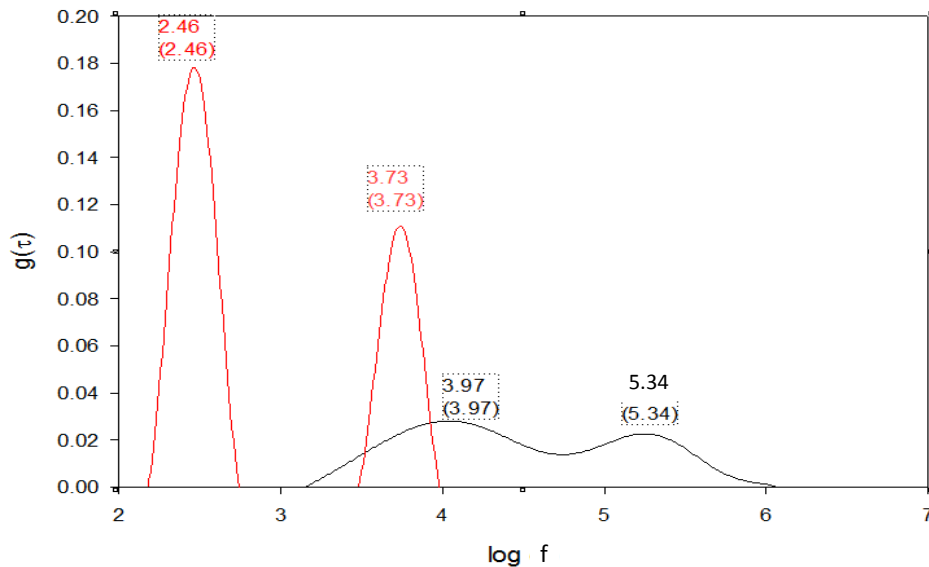


Fig 6 – The DRT analysis with large dispersion in the time-constants of the processes shows broad and shallow distribution peaks. The Rs(RQ)(RQ) synthetic data is used in two sets of analysis but the degree of dispersion in the time constants has been changed - The shape peaks in the red distribution line shows peaks from CPE-p values of 0.95 for both processes. In the second case (black line), the CPE-p value of 0.7 and 0.65 was used and the DRT analysis has resulted into broad peaks.

	Parameter	Description	Default value	Best value	Remarks
1	NS	no of points where f should be calculated	60	1000	computational time increase with increasing NS. Do not use higher than 1000 if not needed. alpha increases?
2	Smin	low end of the tau	data dependent	use the calculated value	Changing this increases the noise and oscillations
3	Smax	high end of the tau	data dependent	use the calculated value	Changing this increases the noise and oscillations
4	DISMOD	whether Tau is a d(lnt) or dt in the kernel eq	1	1	
5	M	no of coefficients in the transformation equation	1	1	just 1 (R0) in our case
6	NS	no of data points	100	60	higher number gives better results
7	NE	no of data sets	1	1	works well with the Zimg data set
8	ERRMOD	Error in the data points	23	23	let program calculate the error
9	ERROR	scaling factor for error	0	0	Use 0 as we are not providing point by point error
10	REGMOD	variant of regularization method(XYZ)	223	223	X = 1 does not work, keep Y=2 always, Z could be relaxed to 2 or 1 if needed
11	LAMBDA	Reg value if you need to define	0	0	ask program to calculate
12	INFMOD	output mode	1	1	output mode (use 1)
13	LAMBST	regularization parameter in log scale	-10	-10	not much impact on the outcome
14	LAMBSP	step size in log scale for reg parameter	1	1	Does impact the results. Start with 1 and go down; less than 1e-3 increases computation time
15	LAMBRP	max deviation of the scaled reg param	12	12	Not much impact
16	LAMBPR	accuracy on a log scale of the scaled reg param	SiEnergy Confidential 1.00E-08	1.00E-01	Use as large as possible to have low oscillation
17	LAMBIT	max num of iteration for calculation	200	200	not much impact by increasing to 1200

Truncated spectrum yields inaccurate results

Data set more points yields better results

Low error data sets preferred

Step size and required accuracy needs to be adjusted based on the data quality

Table I - The impact of the program parameters on the outcome was studied by systematically varying the parameters. The key parameters are shown on the right side.

6. Difficulties arising in the calculations using data sets from real experiments –

The following four (4) parameters were identified as the key for a meaningful relaxation spectrum in the calculation of relaxation spectrum using data sets from real experiments – a) no of data points in each spectrum, b) data sets over 1 Hz to 2 MHz which covers all the relaxation processes in SiE button cells completely, c) Low noise in SiE data sets which clearly shows a large data error at two separate regions in the spectra, and d) program parameter, LAMBPR, which controls the required accuracy for the given data set with specific noise, distribution and regularization parameter(6). The publication which especially deals with the difficulties in the calculations of the distribution of relaxation times from the “real experimental data sets” was consulted and often used as a guide in reaching final decision:

- a. **No of data points, n** – The authors have suggested that the *results become better with increasing number n of data points* (7). The FTIKREG program data sample files contained 200 data points each and the examples files for demonstration in publication used as many as 600 data points in the calculation. In contrast, the std SiE button cell impedance data files contain only 60 points. Unsuccessful attempts were made to calculate distribution spectra from 60 data points (see below). However, knowing that increasing the data points imposes a penalty in terms of acquisition time during the experiments, the data points could not be increased to a large number. An arbitrary number of 120 was chosen for all the impedance work. No systematic study was undertaken to evaluate the impact of increasing number points on the results at this time. The data acquisition increased from ~2 min to ~4 min when the data points were increased from 60 to 120 for each spectrum.
- b. **Incomplete data sets with transition region** - The calculation of distribution spectrum for data with only terminal and plateau region was rather straightforward. The data sets which include transition regions could be analyzed. The authors clearly demonstrate this anomaly of the program with a data set which contains a transition region. In such case, the analysis needs to be performed with a smaller data set after removing data related to the transition region (7). A number of impedance data sets acquired from SiE button cells were examined and it was concluded that in order to cover all the peaks, the impedance data in the range of 1 Hz to 2 M Hz needs to be collected. The data acquisition program was changed accordingly.
- c. **Noise in the data points** - The authors have suggested that the *results become better with decreasing data error, $\sigma(\omega)$* . The visual inspection of SiE data sets clearly shows a large data error at two separate regions in the spectra - at low frequency end (< 30 Hz) and an unexplained upward swing at high frequencies (> 40 kHz) (Fig 7). Eliminating data points was not a

viable option as the analysis requires equally spaced data points (7). Two different strategies were devised to overcome this shortcoming. The sources of this noise were identified - a) The low frequency noise is mainly originating from poor isolation sample signals from the current flowing in heater circuit. No attempt was made to minimize or eliminate such noise during the course of this study, but two level filtering was used to correct and filter the data in the low frequency region (described below). b) The high frequency error is caused by the combination of measurement instrument and the high frequency data was eliminated beyond 40 KHz and an extrapolated sub set of data was appended to each data set such a complete set till 2 M Hz is always present for a correct analysis (Fig 8). The strategy used in the filtering and extrapolation will be discussed in the subsequent sections.

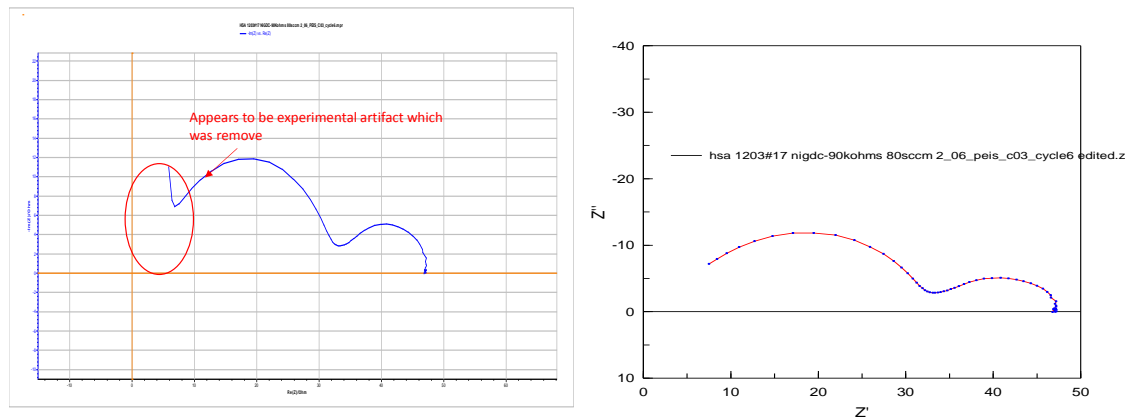


Fig 7 - A typical LT NiGDC spectrum showing upward swing at high frequencies and large noise at low frequencies. Special strategies were devised to overcome the difficulty in the analysis (see text).

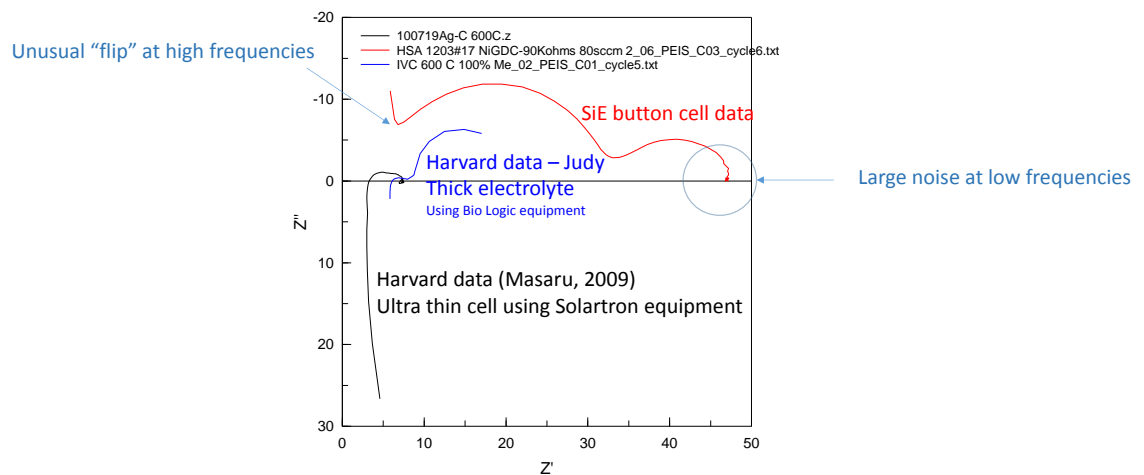


Fig 8 - Impedance spectra from various SOFCs. The SiE button cell exhibits a strange up swing due to interference from the measurement instrument and the heater circuit.

- d. **Data correction using EXCEL add-in MPOC (Manipulating Points on Chart)** – The low frequency noisy data was corrected by hand using an EXCEL add-in (see below). Once again, no systematic study was not performed but visual inspection was used as a guide to correct data sets. The data at the frequencies were passed through a digital filtering step before analysis (described low).

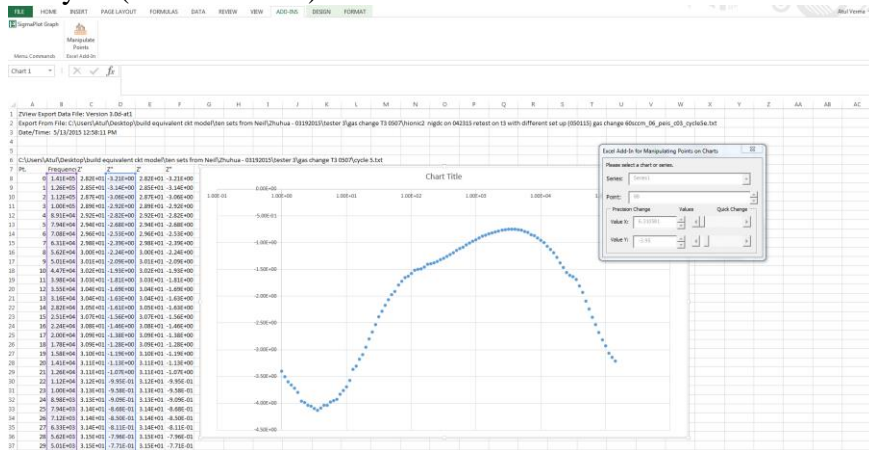
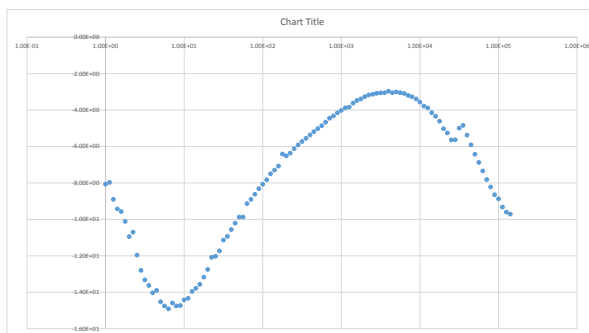
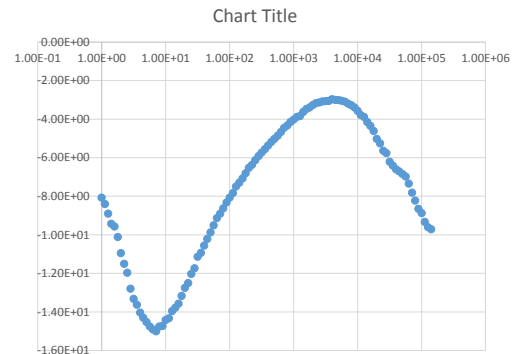


Fig 9 - Screen shot of a typical manipulation using EXCEL add-in MPOC.

- e. **Data Filtering** – After correcting the low frequency data by hand, the data was passes through a filtering step. Three different types of digital filtering routines were examined – a) Moving Average, b) Savitzky–Golay filter, and c) Loess filter (<http://www.mathworks.com/help/curvefit/smoothing-data.html?searchHighlight=Loess>) - Loess filtering was picked to filter data in the low frequency range based on the nature of noise in SiE button cell data sets and robustness of Loess digital. No systematic study was conducted at this time.



Before



After

Fig 10 - The imaginary component of the measured impedance, Z_{img} , before (left) and after (right) data filtering. Pl note that both, MPOC and Loess filtering has been used to clean up the noise.

- f. **Time required to complete analysis of each spectra** - The time required for analysis of each set is estimated to be 45 min and currently thirteen (13) cycles are being acquired to assess the degradation behavior of each button cell. The data preparation (formatting, extrapolation and filtering) for the DRT analysis was found to be most lengthy step which takes about 30 min for each set. Although the computation time was limited to less than 2 min, the overall analysis and visualization time was in the order of 15 min (The data needs to be moved between EC_LAB, ZVIEW, EXCEL, FORTRAN (DOS), EXCEL and Sigma Plot) An integrated Mathcad (or Octave, a free Mat lab alternative) platform has been suggested which is expected to cut down the analysis time by 1/3.
 - g. **Sample-to-Sample variation** – As a physio-chemical model for ultra-thin SOFC does not exist currently, the accuracy of the model are solely assessed on the consistency of results. The sample – to – sample variation has been main impediment during the development of this tool. The current general model for SiE cells has been reached through searching for repeating patterns in the distribution spectra from a limited sample size.
7. **Analysis of Low Temperature Ni-GDC (LT- NiGDC Cells) deposited anode cells** - The general pattern of impedance as seen in the Nyquist plot appears quite similar (Fig 11) among cells. The pattern includes a broad high frequency depressed semi-circle and a second lower frequency broad semi-circle which has a “straight-ist” component at the right-hand side. As seen in the plots below (Fig 12), there is a definite sample to sample variation in the magnitude of the associated resistances (and capacitances). The DRT analysis shows five (5) relaxation processes which could be associated with a LT-NiGDC Cell. The time dependence of these relaxations was also analyzed to investigate the degradation pattern in the cells (Fig 13,14). The number of relaxation processes and their peak frequencies were used in the equivalent circuit modeling. The associated resistances were calculated using CNLS fittings and finally, the time dependent changes in the resistances were plotted (Fig 15). The overall cell degradation behavior could be divided into two different regions - 1) Rapid degradation region observed in $t = 0$ to $t = \sim 4$ hrs. and b) Slow degradation region observed for $t > \text{hrs}$. The degradation rates of individual processes were not calculated and the mechanism of degradation was not investigated.

The degradation rates among samples is quite different as seen in the time evolution of the impedance of three samples below (Fig 16).

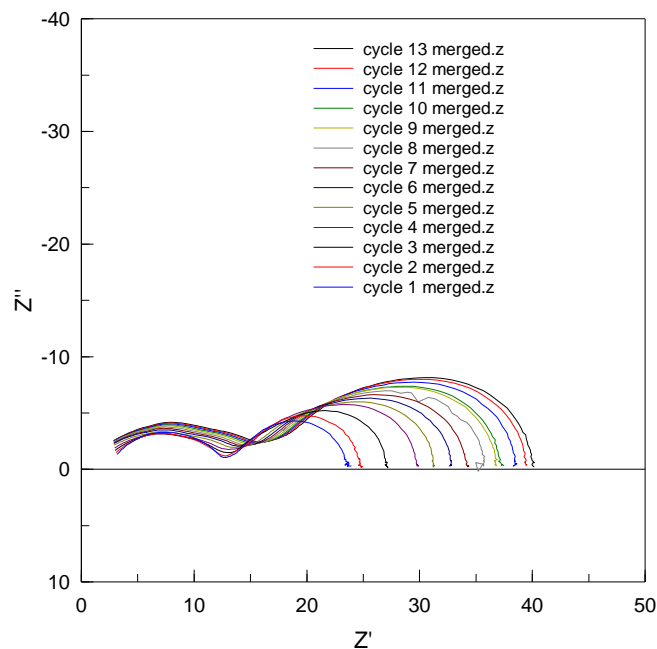


Fig 12 - A typical impedance behavior exhibited by low temperature deposited Ni/GDC cell showing two distinct relaxation processes. The left side of the low frequency process shows a straight-ish region.

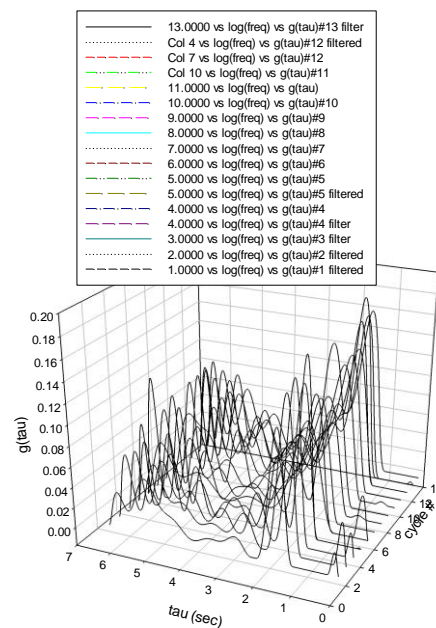
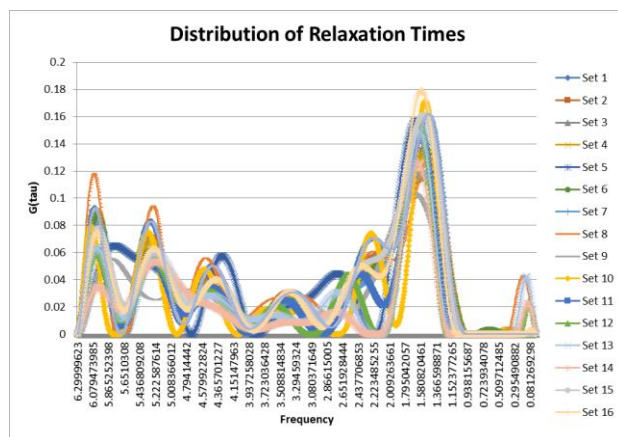


Fig 13 - The time dependence of five (5) distribution peaks as a function of time. The peak positions are more or less at the same location of the peak height changes as the resistance contribution from processes change with time.

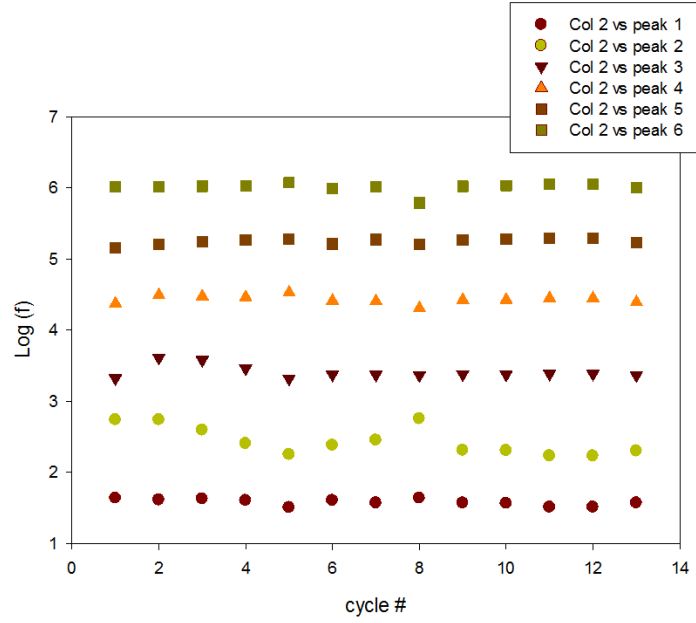


Fig 14 - The time dependence of five (5) distribution peaks as a function of time. The peak positions are more or less at the same location of the peak height changes as the resistance contribution from processes change with time (the cycle 8 data has been influenced by larger noise in the data set)

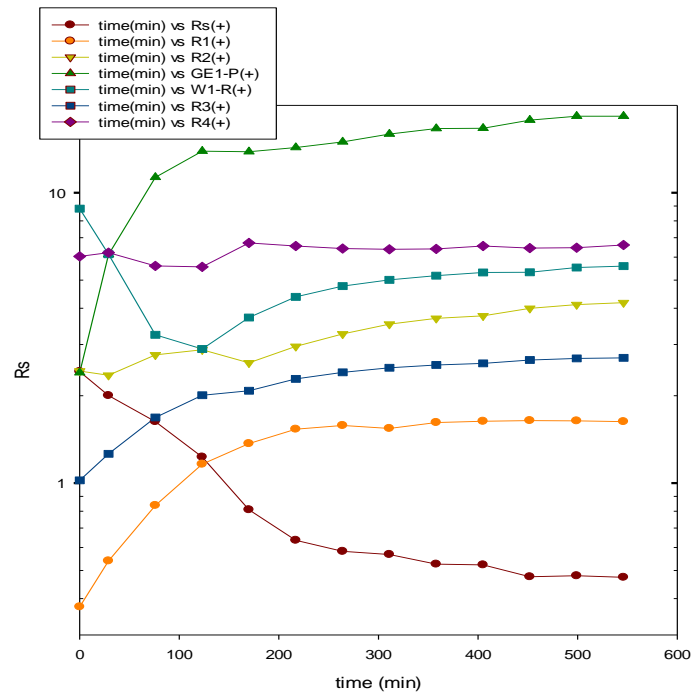


Fig 15 - The time dependence of various resistances associated with the each processes for a LT-NiGDC sample.

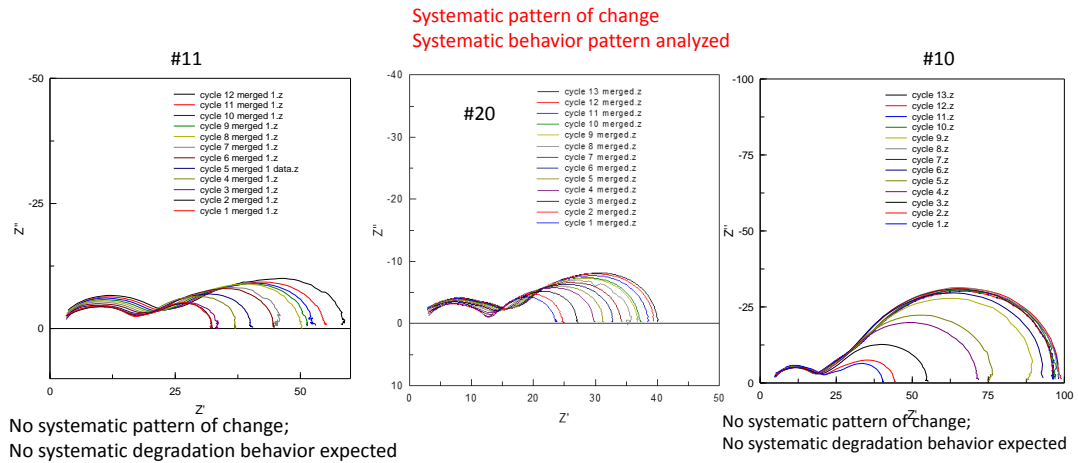


Fig 16 - The degradation behavior among the same batch of cells was not consistent. Cell#20 shows a systematic monotonous behavior (Fig 15) but cell #11 and 10 show no systematic behavior.

8. **Analysis of High Temperature Ni-GDC (HT- NiGDC Cells) deposited anode cells** - The general pattern of impedance as seen in the Nyquest plot appears quite similar (Fig 17) among cells which are deposited at high temperature. However, there is a clear difference in their impedance fingerprint compared to LT-NiGDC cells. HT-NiGDC cells has a much smaller high frequency depressed semi-circle and a second low frequency broad semi-circle does not have any “straight-ist” component at the right-hand side. The DRT analysis shows five (5) relaxation processes which could be associated with a HT-NiGDC Cell. The associated resistances were calculated using CNLS fittings and finally, the time dependent changes in the resistances were plotted (Fig 18). The overall cell degradation behavior could be divided into two different regions - 1) Rapid degradation region observed in $t = 0$ to $t = \sim 1/2$ hrs. and b) Slow degradation region observed for $t > 1/2$ hrs. The degradation rates of individual processes were also calculated and the mechanism of degradation was investigated using gas change experiments.

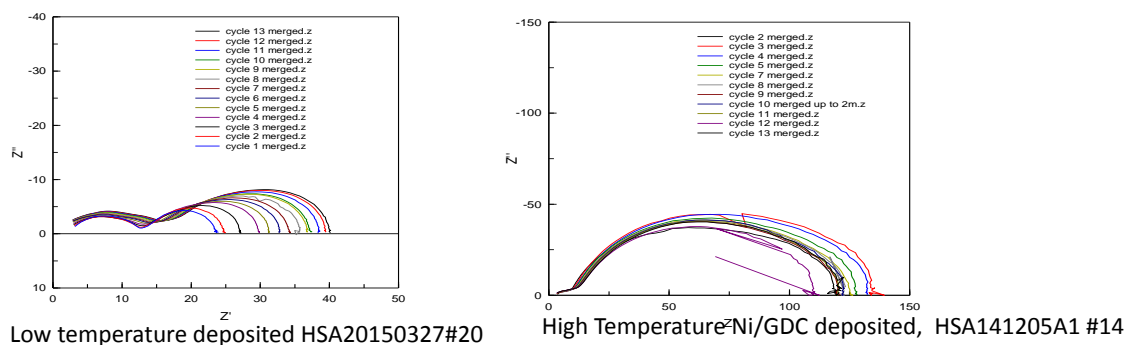


Fig 17 - The impedance plot of high temperature deposited Ni-GDC (HT-NiGDC, shown on the right side) shows a distinctly different impedance fingerprint compare to LT-NiGDC (left side).

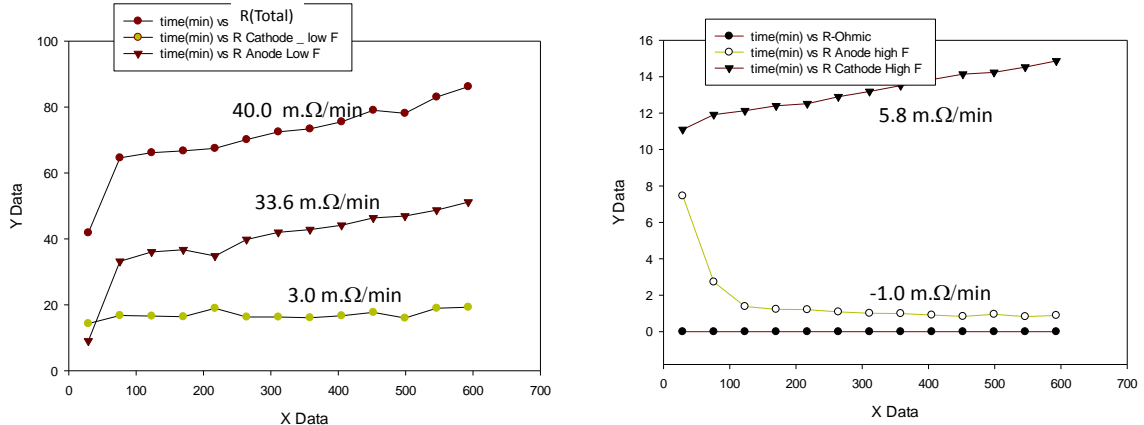


Fig 18 - The resistances associated with all five processes were calculated and plotted as a function of time. ~80% of degradation can be attributed to an anode related process (see text).

9. **Peak assignment** - The individual processes in the DRT spectrum were identified with help of the gas change experiments. A series of impedance measurements were performed by systematically changing gas composition in the anode and cathode compartments. As seen in Fig 19, the peaks at 105.4 and 101.1 clearly respond to the change in the cathode composition which was varied from air (21% O₂) to 100% O₂. Similarly, the anode gas composition was also changed from 100% H₂ to 52.5% H₂ and the response in the peak associated with anode was observed (Fig 20). Based on these gas change experiments a tentative assignment of the peaks has been made -

- Peak at $\log f = \sim 5.4$ is related to cathode – called Cathode Hf peak (CHF) fits simple (RQ) model
- Peak at $\log f = \sim 1.1$ is related to cathode – called Cathode Lf peak (CLF) fits a simple (RQ) better than G (Gerischer) impedance
- Peak at $\log f = \sim 4.5$ is related to anode – called Anode Hf peak (AHF) fits simple (RQ) model
- Peak at $\log f = \sim 2.3$ is related to anode – called Anode Lf peak (ALF) fits simple (RQ) model

Please note that the high frequency processes are often found lumped together. As the accuracy of data is quite poor in the high frequency region, the peak location and magnitude of related impedances are difficult to extract. A fifth peak which happen to be small in magnitude ($R < 0.1$ ohms) was sometimes found buried in the high frequency end. All together four (3 cathode gas change and one anode gas) gas change experiments were performed and consistent peak response was observed.

It is suggested that additional verification gas change runs are performed. In order to develop a detailed mechanistic understanding experimental parameters (sample active area, thickness, gas compositions, temperature and DC bias) need to be varied systematically

and their impact on cell component needs to be studied (Table II). Such a study will be useful in constructing a detailed physio-chemical model for SiE cells.

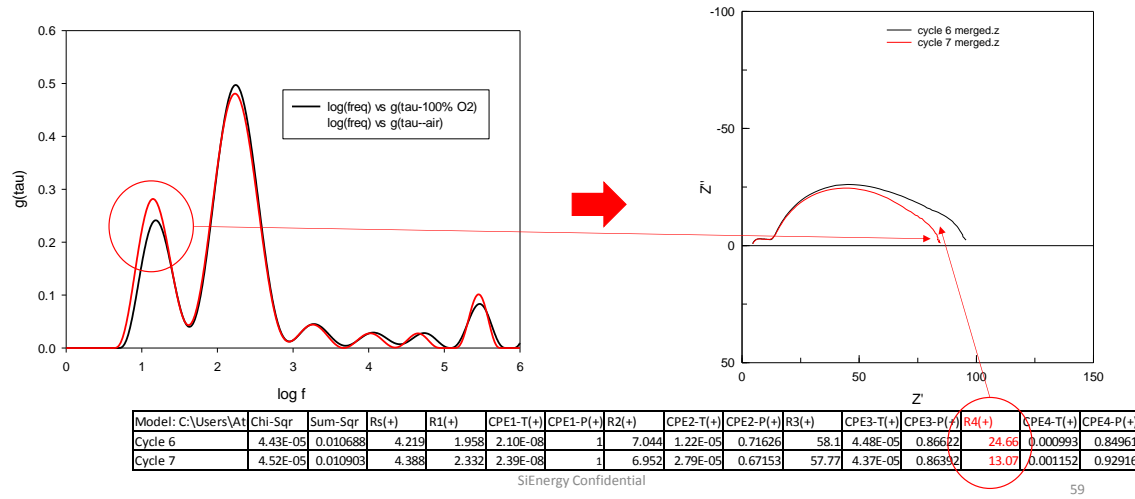


Fig 19 - The DRT plot of a cathode gas experiment showing impact of gas change on peak at $10^{1.1}$ and $10^{5.4}$. These two peaks were attributed to cathode related processes and other three peaks were attributed to anode processes.

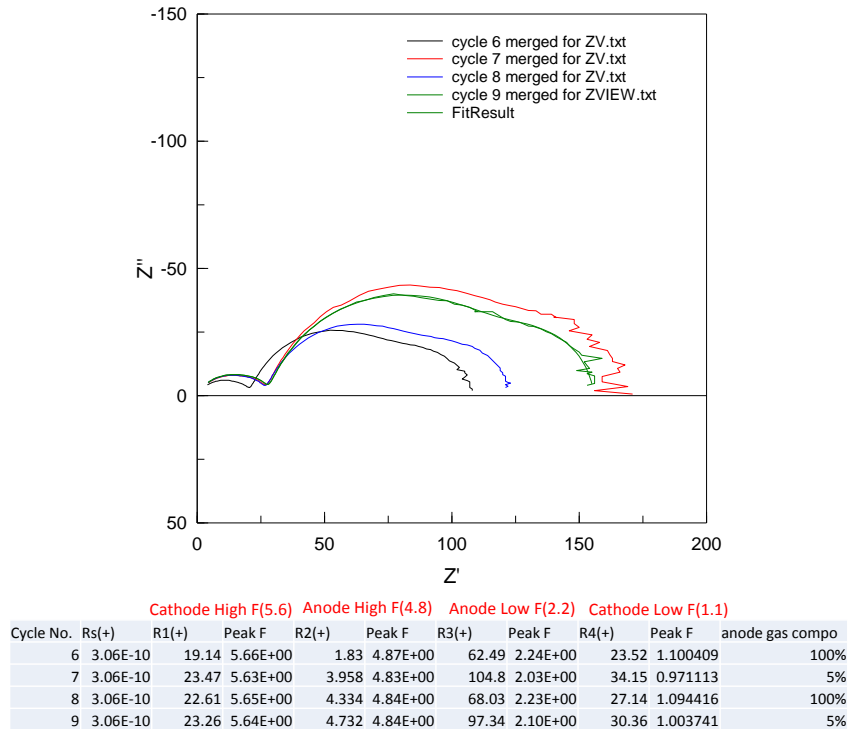


Fig 20 - The impedance plots of an anode gas change experiment with calculated peak frequencies show that the peaks at $10^{4.8}$ and $10^{2.2}$ Hz is related to anode process. The contribution from the third anode processes is often very small and it is not visible in this case.

Variables	Description	Expected Outcome	Experimental space	Expected impact on the understanding and on deconvolution	Experimental difficulty level (low, medium, high)	Order of experiment (high, medium, low)	Status
sample area	Variation in the electrochemical active area of the operating FC;	The component resistance is expected to scale with the size; anode performance may have some influence as the current path changes	dot cell, button cell coupons, single cell, etc.	medium	low	medium	some data available for testing
layer thicknesses	Vary the layer (cathode, electrolyte, anode) thicknesses	The electrolyte resistance is expected to scale with the thickness. The surface controlled processes (cathode and may be anode) are not expected to scale with the thicknesses	2-3X change in the thickness can be achieved	medium	low	medium	no data
Temperature	Vary cell temperature	Thermally activated processes are expected to show large change (electrolyte resistance, charge transfer process). The gas diffusion process is not expected to have much temperature dependence.	450 - 550 C at 25 C steps	high	low	medium	no data
DC bias	Vary the DC bias under which the impedance data is to be collected	Electrode activation polarization processes are expected to have large dc bias dependence.	0.1 to 0.5 V	high	low	High	some data available for testing
Current density	Vary the current under which the impedance data is being collected	The polarization processes are expected to be functions of currents - activation polarization, mass transport limiting polarization	0 to 200 mA/cm ²	medium	low	low	no data
Anode H ₂ concentration	Vary the anode gas composition (H ₂ /N ₂ ratio)	Anode processes are expected to be impacted by the anode gas composition - H ₂ adsorption process will be a function of H ₂ concentration.	5 - 100% H ₂	high	low	High (use 5% and 100% H ₂)	some data available for testing
Anode H ₂ O concentration	Vary the water content in the anode gas	Anode processes are expected to be impacted by the anode gas composition - H ₂ O desorption process is expected to be a function of PH ₂ O. Ni dissolution and transport will be a function of H ₂ O especially at higher temps.	0 - 3% H ₂ O	high	low	High (use 0% and 3%)	no data
Cathode O ₂ concentration	Vary the oxygen content in the cathode gas	Cathode processes are expected to be impacted by the cathode gas composition - adsorption process will be a function of gas composition	1 to 100 % O ₂	high	low	High (use 21% and ~100%)	some data available for testing
Cathode H ₂ O concentration	Vary H ₂ O content in the cathode gas	Cathode processes are expected to be impacted by the water content in the cathode gas (water dependence has been reported for LSM cathodes). Sr-hydroxide formation and degradation could be a factor.	0 - 3% H ₂ O	low	high	low	no data
Cathode quality	Good cathode vs bad cathode cells	The mechanism of oxygen reduction could drastically change - f - from surface controlled to diffusion controlled. YSZ layer instead of LSCF cathode layer is expected to exhibit poor performance (conceived by Neil)	good/bad	high	medium	medium (use YSZ cathodes)	no data
Anode quality	Good anode vs bad anode	Non catalytic element in the anode could have major influence on the reaction rate and on anode performance. The mode of reaction could change.	good/bad	medium	high	low	no data

Table II- List of experimental variables for proposed impedance experiment in order to conduct a complete physio-chemical model of SiE cells.

10. Outstanding issues/Pending work –

- Hardware related** - The noise at the low and high frequency-end which limits the accuracy of the analysis needs to be reduced. Two different sources have been identified as the key cause for the observed noise – a) The current design of heater and sample holder is causing large noise in the impedance data which needs to be minimized, b) There seems to be some noise caused by the interference from the inherent sample (and jig including wiring etc.) and the impedance of the measurement equipment itself (see below). The high frequency range of the useful data was extended by replacing the measurement equipment (see below).
- Software related** – The current methodology for analysis uses a number of commercial software tools and data needs to be formatted and moved between these software tools. An integrated software will eliminate such time-consuming steps and will help in cutting down the overall analysis time.
- Noise in the analysis due to sample-to-sample variation** – Extra caution should be taken in drawing conclusions knowing the inherent sample-to-sample variation in SiE button cells. Appropriate sample size needs to be tested before drawing any meaningful conclusion/s.




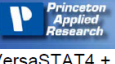


11. Proposed Future Development and Future Experiments -

- Automate the analysis steps** – An integrated software tool needs to be developed which will cut down the analysis time. As a number of samples

will be needed for meaningful conclusions cutting down the crucial analysis time will be important.

- b. **Improve the hardware** – The sample heater which causes large noise in the data needs to be re-designed. Superior quality impedance equipment will help in collecting high quality data sets.

Electrochemical Impedance Spectroscopy for Stacks Testing Equipment

3 kW _{el} SOFC stack 60 cells a 100 cm ² U _{stack} = 42 V I _{stack} = 71.4 A	 target values	 1260/1287 + Power Booster	 IM6 + PP 2xx	 VersaSTAT4 + Power Booster	 CLB 500	 TrueData-EIS
frequency range	1 mHz ... 1 MHz	10 µHz ... 100 kHz	10 µHz ... 200 kHz	(10 µHz ... 1 MHz)	10 µHz ... 10 kHz	200 µHz ... 100 kHz
impedance range	0.1 ... 100 mΩ	10 µΩ ... 1 kΩ	1 µΩ ... 1 kΩ	n.s.	n.s.	0.1 mΩ ... 15 Ω
accuracy (error at 1 mΩ / 100 kHz)	1 %	30 % / 30° (@ 10 mΩ)	0.25 % (f, Z not specified)	n.s.	2 % / 2°	1 % / 1°
max. bias voltage [V]	100	50	± 5 / 10 / 20	20	10	300
max. bias current [A]	100	25	± 40 / 20 / 10	20	50	1000
max. power diss. [kW]	3	0.125	0.25	n.s.	0.5	150

→ limitations due to the testing equipment

- c. **Perform detailed experiments with systematic variation in the experimental parameters** – In order to develop a detailed mechanistic understanding experimental parameters (sample active area, thickness, gas compositions, temperature and DC bias) need to be varied systematically and their impact on cell component needs to be studied. Such a study will be useful in constructing a detailed physio-chemical model for SiE cells.
- d. **Perform model studies on model systems to understand the limitation of the technique and analysis methodology** – Use commercial cells (such as thick substrate NexTech cells) to verify the technique and methodology. Such as study will also help in understanding the limitations and boundaries of the technique.

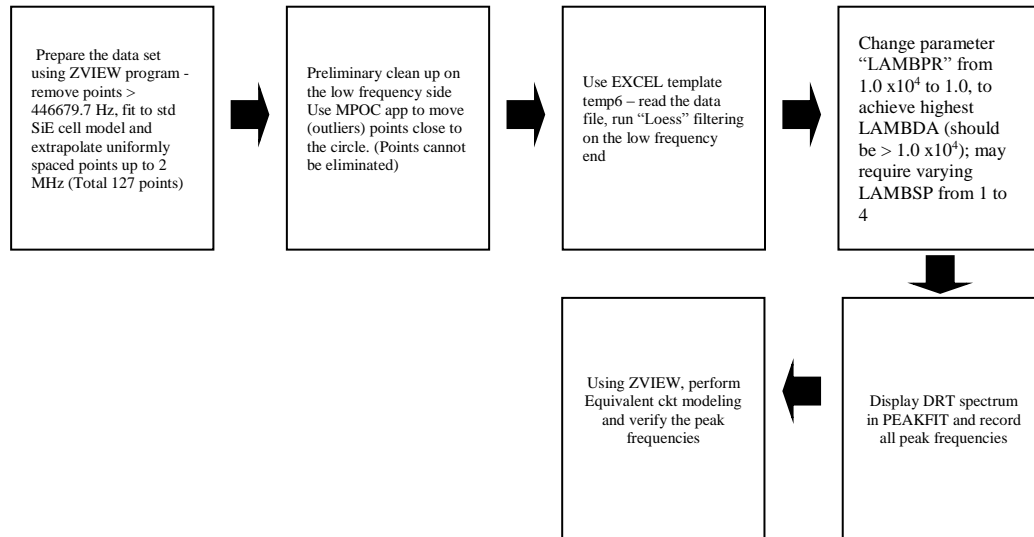
References

1. J.R. Macdonald, Impedance spectroscopy, Wiley Interscience, New York (1987).
2. B.A. Boukamp, Solid State Ionics, 20, 31 (1986).
3. M.E. Orazem, and B. Tribollett, Electrochemical Impedance Spectroscopy, John Wiley & Sons, New York (2008).
4. D. Johnson, “ZView Electrochemical Impedance Software, Version 3.2b”, Scribner Associates, Inc. (2008).
5. J. Weese. A Reliable and Fast Method for the Solution of Fredholm Integral Equations of the First Kind based on Tikhonov Regularization. Computer Physics Communications, 69(1):99–111, (1992).

6. User Manual FTIKREG: A program for the solution of Fredholm integral equations of the first kind, (2008).
7. C. Elster, Prof. Dr. J. Honerkamp, J. Weese, Using regularization methods for the determination of relaxation and retardation spectra of polymeric liquids, *Rheologica Acta*, March/April, Volume 31, Issue 2, pp 161-174, (1992).
8. J. Honerkamp and J. Weese, Tikhonov's regularisation method for ill posed problems, *Continuum Mech. Thermodyn.* 2, 17 (1990).
9. J. Winterhalter D. G. Ebling, D. Maier and J. Honerkamp, An improved analysis of admittance data for high resistivity materials by a nonlinear regularization method, *J. Appl. Phys.* 82, 5488 (1997).
10. H. Schichlein. A.C. Müller, M. Voigts, A. Krügel, and E. Ivers-Tiffée, *J. Appl. Electrochem.*, 32, 875 (2002).
11. Leonide, V. Sonn, A. Weber and E. Ivers-Tiffée, "Evaluation and modeling of the Cell resistance in anode-supported solid oxide fuel cells", *J. Electrochem. Soc.*, 155, pp. B36-B41 (2008).
12. V. Sonn, A. Leonide and E. Ivers-Tiffée, "Combined Deconvolution and CNLS Fitting Approach Applied on the Impedance Response of Technical Ni/8YSZ Cermet Electrodes", *J. Electrochem. Soc.*, 155, pp. B675-B679 (2008).
13. Leonide, SOFC Modelling and Parameter Identification by means of Impedance Spectroscopy, Ph.D Thesis, KIT Publishing, Karlsruhe (2010).
14. Alexander Kromp, Model-based Interpretation of the Performance and Degradation of Reformate Fueled Solid Oxide Fuel Cells, Ph.D Thesis, KIT Publishing, Karlsruhe (2014).

Appendix

STEP BY STEP PROCEDURE FOR DRT ANALYSIS



1. Copy the data set from EC_CON computer
2. Record the details of the cell (processing condition and testing condition, OCV and power degradation etc.) in the master sheet
3. Data file preparation - Keep same no of points in the DRT data file (maintain same frequencies in each data file) –
 - a) Total number points collected from 1 Hz to 1×10^6 = 121
 - b) Points removed from the high frequency end (the erroneous high frequency tail points) = 8 (remove from 4.466797×10^5 to 1×10^6)
 - c) Points added by extrapolating in the high frequency range = 14 (from 4.466797×10^5 to 2×10^6)
 - d) Total number of points in each data file = 127
4. USING EC LAB
 - a) Extract various cycles (use only under load data) using EC LAB
 - b) Export (as txt file) each cycle to the appropriate folder
5. USING ZVIEW
 - a) Examine the data – write notes and remarks on the master sheet
 - b) Extrapolation procedure –
 1. Eliminate high frequency end (chop off 4.466797×10^5 and higher) and save the edited data set
 2. Fit data to a five (or four) sub circuit model – record the fitted parameters
 3. Simulate data between 4.466797×10^5 and 4.466797×10^{10}
 4. Save the simulated data; merge the simulated data to the raw data and re save as "Z" file and export as raw data
6. Open the raw data in EXCEL - fix the outliers manually; use MPOC add-in and resave
7. Change R_0 in the FTIKREG Fortran program, recompile

8. Run Template v6.XLS and FTIKREG to analyze the data set (change parameters to achieve highest possible lambda, mainly LAMBSP CHANGE FROM 1 TO 4)
9. Transfer data (SOL file) to Peakfit; Run Peakfit and record the f_{\max} in the EXCEL sheet
10. Optional - Analyze the data in ZVIEW using new information (no of peaks and peaks frequencies, f_{\max})
11. Record the findings in the master excel sheet
12. PERFORM FTIKREG VERFICATION RUNS WITH SYNTHETIC DATA SETS GENERATED USING modelled equivalent circuit

THE USE OF REGULARIZATION METHODS FOR EVALUATING FUEL CELL ELECTRODES

Volker Sonn and Ellen Ivers-Tiffée
Institut für Werkstoffe der Elektrotechnik
Universität Karlsruhe /TH
D-76131 Karlsruhe / Germany
Email: Volker.sonn@iwe.uni-karlsruhe.de

Keywords: Impedance Spectroscopy, Regularisation Methods, SOFC Cermet Anodes

Introduction

Due to the great number of physico-chemical processes and the complex topology of the electrode /electrolyte interface, a comprehensive model describing SOFC electrodes is not available at present. As a result, the main characterization method, the electrochemical impedance spectroscopy (EIS), cannot tap his full potential with a model based approach. Not only to understand the complex processes inside SOFC electrodes but also to deploy new application, e.g. in-situ diagnosis of fuel cells based on EIS, new ways of analysing impedance_data have to complement the established methods.

Distribution of Relaxation Times

By assuming an equivalent circuit, one is committed to a certain number and type of dispersion processes in the cell. An alternative to this approach is the use of an arbitrary distribution of relaxation times. In this representation, a dynamic process in the system is represented by a peak, and the area under the peak equals the polarisation resistance caused by the under laying loss mechanisms.

In order to determine the distribution function from the experimentally determined values of Z , one has to solve Eq. 1 for $g(\tau)$,

$$Z_{pol}(\omega) = \int_0^{\infty} \frac{g(\tau)}{1 + j\omega\tau} d\tau + R_0 \quad (1)$$

where R_0 reflects the pure ohmic resistance. Solving this equation is a rather unpleasant problem, because Eq. 1 is a Fredholm Integral of the first kind, and its inversion is severely ill-posed. Therefore, the solution is extremely sensitive to noise-induced errors in Z . To stabilize the solution a Tikhonov-Regularisation [1] can be used, which allows the inversion of Eq. 1 while simultaneously determining R_0 .

Experiments

The model equation (Eq.1) was applied to the impedance data from symmetrical Ni/10ScSZ anodes (volume ratio 50:50, $d_{50}=0.8\mu\text{m}$). The cells were characterised under different operating conditions (temperature, overvoltage, humidification and fuel gas composition) in between 100 mHz...300 kHz with a Zahner IM6 impedance analyser. The relaxation spectra were calculated from Eq. [1] by using the FTIKREG [2] program.

Results and Discussion

Fig. 1 shows the impedance spectra of a Ni/SSZ anode and the resulting DRT at different humidifications: It is possible to get a stable resolution of up to 5 processes, which show a decided dependence on the operating conditions. Process 1 is related to a gas diffusion process outside the cermet of the anode. The processes P2-P4 are related to the charge transfer reaction. The dominant peak of P3 shows a distinct dependence on the partial pressure of H_2O . This main process accelerates (shift towards higher frequencies) with the amount of water in the fuel gas. Simultaneously the polarisation resistance decreases until both parameters reverse their trends for high $p(\text{H}_2\text{O})$.

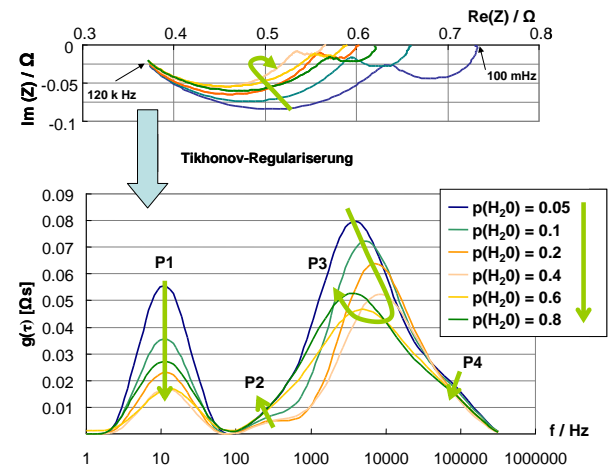


Figure 1. Impedance data and resulting relaxation spectra of an Ni/SSZ-Cermet anode at different $p(\text{H}_2\text{O})$.

Conclusions

The distribution of relaxation times is an extreme powerful concept for evaluating fuel cell electrodes, in case that no detailed model is available or the predefinition of a single model does not fulfil the intention of the measurement. A drawback is, since the calculation of the DRT is ill-posed, it relies on low-noise impedance data and requires the use of regularisation methods. Evaluating the impedance of a Ni/10ScSZ by means of the Tikhonov-regularisation we were able to achieve a stable resolution of 5 processes.

- [1] A.N. Tikhonov, V.Y. Arsenin, Solution of ill-posed Problems, Winston and Sons, Washington DC, 1987
- [2] J. Weese; Comp. Phys. Comm. 69 99-111 (1992)

A reliable and fast method for the solution of Fredholm integral equations of the first kind based on Tikhonov regularization

Jürgen Weese

Freiburger Materialforschungszentrum F.M.F, Stefan-Meier-Straße 31, W-7800 Freiburg im Breisgau, Germany

Received 8 March 1991; in revised form 11 July 1991

In many physical and chemical applications one is faced with the problem of calculating the solution of a Fredholm integral equation of the first kind from noisy experimental data. For such problems a solution method based on Tikhonov regularization together with the computer program FTIKREG is presented. In contrast to other solution methods which are based on Tikhonov regularization especially the determination of the regularization parameter has been improved. This improvement leads to much better results, because the error of the result depends mainly on the regularization parameter. Also the numerical effort needed for the corresponding calculation is small for the proposed method. As a consequence many problems can be solved with the program FTIKREG on a personal computer. In order to illustrate the most important features of the solution method, the program FTIKREG is applied to simulated data.

PROGRAM SUMMARY

Title of program: FTIKREG (for Fast TIKhonov REGulariza-
tion)

Catalogue number: ACGH

Program obtainable from: CPC Program Library, Queen's
University of Belfast, N. Ireland, (see application form in this
issue)

Licensing provisions: none

Computer: (i) Sun SPARCstation I, (ii) 386SX PC

Operating system: (i) Unix, (ii) MS-DOS

Programming language used: FORTRAN 77

Memory required to execute with typical data: 2 MB

No. of bits in a word: 32

No. of lines in distributed program, including test data, etc.:
4343

Separate documentation available: User Manual; *no. of pages:*
21

Keywords: Fredholm integral equation of the first kind,
ill-posed problem, Tikhonov regularization

Nature of physical problem

Experimental not accessible functions and distributions are often related to an experimental accessible quantity by a Fredholm integral equation of the first kind. Therefore the solution of the integral equation must be calculated from noisy experimental data, in order to determine such a function or distribution.

Method of solution

The solution method is based on Tikhonov regularization [1]. For the determination of the regularization parameter the SC-method [2] is used.

Typical running time

For a large number n of data points the running time is proportional to nn_s^2 . Thereby n_s denotes the number of points at which the result is calculated. For a small number n of data points the running time is proportional to n_s^3 .

References

- [1] C.W. Groetsch, The Theory of Tikhonov Regularization for Fredholm Equations of the First Kind (Pitman, London 1984).
- [2] J. Honerkamp and J. Weese, Continuum Mech. Thermo-
dyn. 2 (1990) 17.

LONG WRITE-UP

Introduction

Often one is interested in quantities which are not directly accessible by experiments, but a relation between these quantities and experimental accessible data is available. Therefore it is necessary to calculate these quantities from experimental data. In the most simple case the relation between the experimental data and the interesting quantities is linear. Assuming, that the errors in the data are Gaussian distributed, this problem can be solved by a least-squares method [1].

A similar problem arises, if a function or distribution which is not directly measurable should be determined. In this case the calculation of the interesting function given experimental data can be very difficult, even if the relation between the function and the data is linear. If for example the relation is given by a Fredholm integral equation of the first kind, difficulties arise, because the solution of a Fredholm integral equation of the first kind is an ill-posed problem (see ref. [2] for the definition of ill-posed problems) and a simple least-squares method is not appropriate for the solution of such a problem [3].

For the solution of Fredholm integral equations of the first kind several methods have been developed [4–7]. From all these methods Tikhonov regularization is the best-known one and there exists much mathematical literature [8] concerning this regularization method. Due to the program CONTIN [9,10] developed by S.W. Provencher, Tikhonov regularization is used in many physical and chemical applications (see e.g. refs. [11,12]). Another well-known and frequently used method (see e.g. ref. [11,13]) for the solution of Fredholm integral equations of the first kind is the maximum-entropy method [6].

When a regularization method is used to calculate the solution of a Fredholm integral equation of the first kind, a value for the so-called regularization parameter must be determined. It depends mainly on this parameter, whether the result obtained by a regularization method is good or not. For this reason procedures for the

determination of this parameter have been developed and studied [14–21].

The procedure for the determination of the regularization parameter is also the main difference between the solution method proposed here and other solution methods. The procedure used here has been introduced in refs. [22,23] as the SC-method (SC for self consistent). References [22,23] also contain a comparison of the SC-method with other procedures which are often used for the determination of the regularization parameter. This comparison leads to the conclusion, that the results obtained with the SC-method are much better and more reliable than the results obtained with the other procedures.

There is another difficulty connected with the determination of the regularization parameter. The procedures used for this purpose require the calculation of intermediate solutions for several values of this parameter, before the final solution is obtained. Every step in this calculation requires matrix inversions, thus the computational effort can be enormous. This difficulty does not arise in the proposed solution method, because a kind of generalized singular-value decomposition [24] is used. As a consequence the computer program FTIKREG which is based on this solution method, also runs on a personal computer.

In the next section a typical problem which arises in many chemical and physical applications is formulated. The result obtained with Tikhonov regularization is defined in section 3, while an efficient way for the calculation of the result is shown in section 4. In section 5 the most important features of the solution method are illustrated. For that purpose the program FTIKREG is used to solve a problem which does arise in the linear theory of viscoelastic fluids.

2. Formulation of the problem

In many chemical and physical applications a function f and m coefficients a_1, \dots, a_m should be determined from data $g_1^\sigma, \dots, g_n^\sigma$ of an experi-

mental accessible function g . These quantities are related by

$$g(t) = \int_{I_s} K(t, s) f(s) ds + \sum_{i=1}^m a_i b_i(t), \quad (1)$$

with functions b_1, \dots, b_m and the kernel function K known from theory. Because of the experimental noise, the data $g_1^\sigma, \dots, g_n^\sigma$ can be considered as realizations of the random variables

$$G_i^\sigma = g(t_i) + \sigma \epsilon_i, \quad i = 1, \dots, n. \quad (2)$$

In this equation $\epsilon_1, \dots, \epsilon_n$ are n independent standard normally distributed random variables, σ is a usually unknown scaling factor of the error and $\sigma_1, \dots, \sigma_n$ are given by an error model. (If e.g. $\sigma_i = 1$, the data are affected by absolute errors of the size σ . If e.g. $\sigma_i = g(t_i)$ the data are affected by relative errors of size σ .) In addition it is frequently known that the function f is positive. In this case the constraints

$$f(s) \geq 0, \quad s \in I_s, \quad (3)$$

must be considered, when the solution of this problem is calculated.

3. Description of the solution method

In the first part of this section, the result obtained with Tikhonov regularization for the problem in section 2 is defined. In this definition the so-called regularization parameter is introduced, which is responsible for the quality of the result given by a regularization method. The procedure used for the determination of an appropriate value for this parameter is described in the second part of this section. In the last part a kind of error interval is introduced. These intervals describe the influence of the data errors on the result.

3.1. Definition of the result

The result obtained with Tikhonov regularization for the problem in section 2 is defined as the

function f_λ^σ and the coefficients $a_1^\sigma, \dots, a_m^\sigma$, which minimize the quantity

$$V(\lambda) = \sum_{i=1}^n \frac{1}{\sigma_i^2} \left(g_i^\sigma - \left(\int_{I_s} K(t_i, s) f(s) ds + \sum_{j=1}^m a_j b_j(t_i) \right) \right)^2 + \lambda \|L f\|_{L_2}^2. \quad (4)$$

In this minimization the constraints (3) must be considered, if the function f is known to be positive. In eq. (4) λ is the so-called regularization parameter, L is an operator, for which the identity or the second derivative is frequently used, and the norm $\| \cdot \|_{L_2}$ is given for an arbitrary function h by

$$\|h\|_{L_2}^2 = \int_{I_s} h^2(s) ds. \quad (5)$$

With an appropriate value for the regularization parameter λ , the first term on the right hand side of eq. (4) forces the result to be compatible with the data. The second term leads to a smooth estimate f_λ^σ of the function f .

In order to get a simple notation, the vector g'^σ , the matrix B' and the operator K' are introduced by

$$g_i'^\sigma = \frac{1}{\sigma_i} g_i^\sigma, \quad i = 1, \dots, n, \quad (6a)$$

$$B_{ij}' = \frac{1}{\sigma_i} b_j(t_i), \quad i = 1, \dots, n, \quad j = 1, \dots, m, \quad (6b)$$

$$(K'f)_i = \frac{1}{\sigma_i} \int_{I_s} K(t_i, s) f(s) ds, \quad i = 1, \dots, n. \quad (6c)$$

Also the coefficients a_1, \dots, a_m and $a_1^\sigma, \dots, a_m^\sigma$ are considered as components of the vectors a and a^σ . With these quantities $V(\lambda)$ can be written as

$$V(\lambda) = \|g'^\sigma - (K'f + B'a)\|^2 + \lambda \|L f\|_{L_2}^2. \quad (7)$$

Thereby $\|v\|$ denotes the Euclidian norm of the vector v .

If no constraints must be considered, the function f_λ^σ and the coefficients $a_1^\sigma, \dots, a_m^\sigma$, given by the minimum of $V(\lambda)$, can be written explicitly as

$$f_\lambda^\sigma = \mathbf{K}'^{-1}(\lambda) \mathbf{g}'^\sigma, \quad (8a)$$

$$\mathbf{a}^\sigma = \mathbf{B}'^{-1}(\lambda) \mathbf{g}'^\sigma, \quad (8b)$$

with $\mathbf{K}'^{-1}(\lambda)$ and $\mathbf{B}'^{-1}(\lambda)$ given by

$$\begin{aligned} \mathbf{K}'^{-1}(\lambda) \\ = (\mathbf{K}'^t(\mathbf{I} - \mathbf{P}_B)\mathbf{K}' + \lambda \mathbf{L}'^t \mathbf{L})^{-1} \mathbf{K}'^t(\mathbf{I} - \mathbf{P}_B), \end{aligned} \quad (9a)$$

$$\mathbf{B}'^{-1}(\lambda) = \mathbf{B}'^+(\mathbf{I} - \mathbf{K}'\mathbf{K}'^{-1}(\lambda)). \quad (9b)$$

The matrix \mathbf{P}_B is the projection into the range of \mathbf{B}' , \mathbf{B}'^+ is the pseudoinverse of \mathbf{B}' and \mathbf{I} denotes a $n \times n$ identity matrix.

If the constraints (3) must be considered, the result can not be written in a similar way.

3.2. Determination of the regularization parameter

As pointed out in the introduction the regularization parameter has a great influence on the result obtained by a regularization method. If this parameter is chosen too small, the function f_λ^σ will show artificial peaks. Otherwise, if this parameter is chosen too large, the function f_λ^σ will be oversmoothed. Thus a good and reliable procedure for the determination of the regularization parameter is necessary.

Such a procedure can be defined by considering the error

$$d_f = \|f - f_\lambda^\sigma\|_{L_2}^2 \quad (10)$$

of the estimate f_λ^σ obtained by Tikhonov regularization. This error is a realization of a random variable denoted by D_f . The expectation value ED_f of this random variable depends on the function f , the regularization parameter λ and the size of the error σ ,

$$ED_f = ED_f(f, \lambda, \sigma), \quad (11)$$

and a good value for the regularization parameter should minimize this quantity:

$$\left. \frac{\partial}{\partial \mu} ED_f(f, \mu, \sigma) \right|_{\mu=\lambda} = 0. \quad (12)$$

Actually, this equation can not be solved in practice, because the function f is not known.

The idea of the SC-method (SC for self consistent) is to replace the function f in eq. (12) by the best estimate which can be obtained from the data. Therefore the function f is replaced by f_λ^σ leading to the equation

$$\left. \frac{\partial}{\partial \mu} ED_f(f_\lambda^\sigma, \mu, \sigma) \right|_{\mu=\lambda} = 0. \quad (13)$$

This equation defines a value λ_{SC} for the regularization parameter. If the value λ_{SC} leads to a good estimate f_λ^σ for the function f , the replacement of the function f by f_λ^σ is justified and eq. (13) should define a good value for the regularization parameter. By solving eq. (13) the regularization parameter is therefore determined in a self-consistent manner.

This method has been proposed in refs. [22,23] and the Monte Carlo simulations in refs. [22,23] have shown that the values for the regularization parameter obtained with this procedure are only slightly different from the optimal value defined by the minimum of $ED_f(f, \lambda, \sigma)$.

To apply the SC-method described so far, the size of the scaling factor σ must be known. However, in many cases this scaling factor is unknown. In order to apply the SC-method in such a case, the scaling factor σ in eq. (13) can be replaced by an appropriate estimate $\hat{\sigma}$.

To get an estimate $\hat{\sigma}$ for the scaling factor σ , one can consider the discrepancy

$$d_g = \|\mathbf{g}'^\sigma - (\mathbf{K}'f_\lambda^\sigma + \mathbf{B}'\mathbf{a}^\sigma)\|^2. \quad (14)$$

The discrepancy d_g is a realization of a random variable denoted by D_g . The expectation value of this random variable depends on the function f , the regularization parameter λ and the scaling factor σ :

$$ED_g = ED_g(f, \lambda, \sigma). \quad (15)$$

With the quantities defined above, an estimate for the scaling factor σ can be defined, by comparing the discrepancy d_g with the expectation value ED_g of the corresponding random variable:

$$d_g = ED_g(f, \lambda, \hat{\sigma}). \quad (16)$$

Again the idea is to replace the function f in eq. (16) by f_λ^σ , because in practice the function f is unknown. Therefore, the estimate $\hat{\sigma}$ for the scaling factor σ is obtained by solving the equation

$$d_g = ED_g(f_\lambda^\sigma, \lambda, \hat{\sigma}). \quad (17)$$

Now the scaling factor σ in eq. (13) can be replaced by the estimate $\hat{\sigma}$ and a value λ_{SC} for the regularization parameter λ is obtained from the equation

$$\left. \frac{\partial}{\partial \mu} ED_f(f_\lambda^\sigma, \mu, \hat{\sigma}) \right|_{\mu=\lambda} = 0. \quad (18)$$

This procedure has been proposed in ref. [23] and the Monte Carlo simulations in ref. [23] have shown that the results obtained with this modification of the SC-method are as good as the results obtained with the SC-method itself. In addition these simulations have shown that $\hat{\sigma}$ is a good estimate for the scaling factor σ .

If no constraints must be considered, explicit expressions can be obtained for the quantities $ED_f(f, \lambda, \sigma)$ and $ED_g(f, \lambda, \sigma)$:

$$\begin{aligned} ED_f(f, \lambda, \sigma) &= \langle \|f - F_\lambda^\sigma\|_{L_2}^2 \rangle \\ &= \|f - \mathbf{K}'^{-1}(\lambda)\mathbf{K}'f\|_{L_2}^2 \\ &\quad + \sigma^2 \text{trace}(\mathbf{K}'^{-1}(\lambda)(\mathbf{K}'^{-1}(\lambda))^t), \end{aligned} \quad (19a)$$

$$\begin{aligned} ED_g(f, \lambda, \sigma) &= \langle \|G'^\sigma - (\mathbf{K}'F_\lambda^\sigma + \mathbf{B}'A^\sigma)\|^2 \rangle \\ &= \|(\mathbf{I} - \mathbf{P}(\lambda))\mathbf{K}'f\|^2 \\ &\quad + \sigma^2 \text{trace}((\mathbf{I} - \mathbf{P}(\lambda))(\mathbf{I} - \mathbf{P}(\lambda))^t). \end{aligned} \quad (19b)$$

Here F_λ^σ , A^σ and G'^σ are the random variables belonging to f_λ^σ , a^σ and g'^σ . $\mathbf{K}'^{-1}(\lambda)$, $\mathbf{B}'^{-1}(\lambda)$ and $\mathbf{P}(\lambda)$ are given by the eqs. (9) and by

$$\mathbf{P}(\lambda) = \mathbf{P}_B + (\mathbf{I} - \mathbf{P}_B)\mathbf{K}'\mathbf{K}'^{-1}(\lambda). \quad (20)$$

If the constraints (3) must be taken into account, the SC-method can not be applied in the way described above, because the expectation values $ED_f(f, \lambda, \sigma)$ and $ED_g(f, \lambda, \sigma)$ can not

be calculated explicitly. Also the numerical evaluation of these two quantities requires too much time. Therefore, the SC-method is modified for this case (see section 4.3).

3.3. Error intervals

A result for a quantity obtained from noisy data is only meaningful, if an information about the influence of the data errors in the result is given. Therefore, in addition to the result, confidence intervals must be calculated. These intervals are usually defined in such a way, that the true value for the quantity is in the interval with a probability of 68%.

The result obtained by a regularization method is affected by two errors, one is a bias caused by the regularization and the other is a statistical error caused by the data error. Because the bias can not be estimated, confidence intervals can not be defined for the result obtained by a regularization method. In spite of this fact, error intervals which describe the influence of the data error for fixed regularization parameter are useful for the interpretation of the result.

Such error intervals can be defined by the influence of additional errors of the size $\sigma\sigma_i$ in the data g_i^σ on the result. If no constraints must be considered, for the function f_λ^σ these intervals are given by

$$\begin{aligned} &[f_\lambda^\sigma(s) - \sigma(f_\lambda^\sigma(s)), f_\lambda^\sigma(s) + \sigma(f_\lambda^\sigma(s))], \\ &\text{with} \\ &\sigma^2(f_\lambda^\sigma(s)) = \sigma^2(\mathbf{K}'^{-1}(\lambda)(\mathbf{K}'^{-1}(\lambda))^t)(s, s). \end{aligned} \quad (21a)$$

The error intervals for the coefficients a_i^σ are given by

$$\begin{aligned} &[a_i^\sigma - \sigma(a_i^\sigma), a_i^\sigma + \sigma(a_i^\sigma)], \\ &\text{with} \\ &\sigma^2(a_i^\sigma) = \sigma^2(\mathbf{B}'^{-1}(\lambda)(\mathbf{B}'^{-1}(\lambda))^t)_{ii}. \end{aligned} \quad (21b)$$

If the constraints (3) must be considered, no explicit expressions for the intervals can be ob-

tained. In addition the calculation of these intervals by a Monte Carlo simulation requires too much time. Therefore, the calculation of the error intervals is simplified in this case (see section 4.3).

4. Determination of the result

In order to determine the result for the problem in section 2, all functions and operators must first be approximated by finite-dimensional vectors and matrices. This step is described in the first part of this section. Then the equations which define the result must be solved. An efficient way to do this, if no constraints must be considered, is shown in the second part of this section. In the last part the modifications necessary to calculate the result with constraints are described.

4.1. Approximation by finite-dimensional quantities

Finite-dimensional vectors and matrices can be introduced for the functions and operators, by approximating the integrals and derivatives by sums and difference coefficients. These approximations can be done in several ways. However, a simple approximation method with a low degree of convergence is sufficient accurate, because the error caused by these approximations is small compared with the error caused by the regularization and the data error. Therefore the quantities $(\mathbf{K}'f)$, $\|\mathbf{L}f\|_{L_2}^2$ and $\|f - f_\lambda^\sigma\|_{L_2}^2$ are approximated by

$$(\mathbf{K}'f)_i \approx \frac{h_s}{\sigma_i} \sum_{j=1}^{n_s} K(t_i, s_j) f(s_j), \quad i = 1, \dots, n, \quad (22a)$$

$$\|\mathbf{L}f\|_{L_2} \approx h_s \sum_{i=1}^{n_l} \left(\sum_{j=1}^{n_s} L_{ij} f(s_j) \right)^2, \quad (22b)$$

$$\|f - f_\lambda^\sigma\|_{L_2}^2 \approx h_s \sum_{j=1}^{n_s} (f(s_j) - f_\lambda^\sigma(s_j))^2, \quad (22c)$$

with

$$s_j = s_{\min} + (j-1)h_s, \quad j = 1, \dots, n_s, \quad (23a)$$

$$h_s = (s_{\max} - s_{\min}) / (n_s - 1). \quad (23b)$$

The values of the coefficients L_{ij} in eq. (22b) depend on the operator \mathbf{L} . If \mathbf{L} is the identity the coefficients L_{ij} are given by

$$L_{ij} = \delta_{ij}, \quad i = 1, \dots, n_l, \quad j = 1, \dots, n_s, \quad (24a)$$

$$n_l = n_s. \quad (24b)$$

If \mathbf{L} is the second derivative the coefficients L_{ij} should be set to

$$L_{ij} = \frac{1}{h_s^2} (\delta_{ij} + \delta_{i(j+2)} - 2\delta_{i(j+1)}), \quad i = 1, \dots, n_l, \quad j = 1, \dots, n_s, \quad (25a)$$

$$n_l = n_s - 2. \quad (25b)$$

If \mathbf{L} is the second derivative and additionally the function f is assumed to vanish smoothly at the upper and lower boundary of the interval $[s_{\min}, s_{\max}]$, the coefficients L_{ij} are given by

$$L_{ij} = \frac{1}{h_s^2} (\delta_{ij} + \delta_{i(j+2)} - 2\delta_{i(j+1)}), \quad i = 1, \dots, n_l, \quad j = 1, \dots, n_s, \quad (26a)$$

$$n_l = n_s + 2. \quad (26b)$$

The coefficients in the eq. (22) can now be considered as elements of the vectors f and f_λ^σ and of the matrices \mathbf{K}' and \mathbf{L}' with elements

$$f_j = f(s_j), \quad j = 1, \dots, n_s, \quad (27a)$$

$$f_{\lambda j}^\sigma = f_\lambda^\sigma(s_j), \quad j = 1, \dots, n_s, \quad (27b)$$

$$K'_{ij} = \frac{h_s}{\sigma_i} K(t_i, s_j), \quad i = 1, \dots, n, \quad j = 1, \dots, n_s, \quad (27c)$$

$$L'_{ij} = \sqrt{h_s} L_{ij}, \quad i = 1, \dots, n_l, \quad j = 1, \dots, n_s. \quad (27d)$$

4.2. Calculation of the result without constraints

The result for the problem in section 2 is defined by the minimum of the quantity $V(\lambda)$.

Using the vector f and the matrices K' and L' this quantity can be written as

$$V(\lambda) = \|g'^\sigma - (K'f + B'a)\|^2 + \lambda \|L'f\|^2. \quad (28)$$

The minimum of $V(\lambda)$ is given by the solution of the equation

$$\begin{aligned} & \left(\begin{pmatrix} B'^t \\ K'^t \end{pmatrix} (B', K') + \lambda \begin{pmatrix} Z'^t \\ L'^t \end{pmatrix} (Z', L') \right) \begin{pmatrix} a^\sigma \\ f_\lambda^\sigma \end{pmatrix} \\ &= \begin{pmatrix} B'^t \\ K'^t \end{pmatrix} g'^\sigma \end{aligned} \quad (29)$$

and can formally be written as

$$\begin{aligned} \begin{pmatrix} a^\sigma \\ f_\lambda^\sigma \end{pmatrix} &= \left(\begin{pmatrix} B'^t \\ K'^t \end{pmatrix} (B', K') \right. \\ &\quad \left. + \lambda \begin{pmatrix} Z'^t \\ L'^t \end{pmatrix} (Z', L') \right)^{-1} \begin{pmatrix} B'^t \\ K'^t \end{pmatrix} g'^\sigma. \end{aligned} \quad (30)$$

By comparing this equation with eqs. (9) and (20), expressions for the quantities $K'^{-1}(\lambda)$, $B'^{-1}(\lambda)$ and $P(\lambda)$ are obtained:

$$\begin{aligned} K'^{-1}(\lambda) &= (Z_f, I_f) \left(\begin{pmatrix} B'^t \\ K'^t \end{pmatrix} (B', K') \right. \\ &\quad \left. + \lambda \begin{pmatrix} Z'^t \\ L'^t \end{pmatrix} (Z', L') \right)^{-1} \begin{pmatrix} B'^t \\ K'^t \end{pmatrix}, \end{aligned} \quad (31a)$$

$$\begin{aligned} B'^{-1}(\lambda) &= (I_a, Z_a) \left(\begin{pmatrix} B'^t \\ K'^t \end{pmatrix} (B', K') \right. \\ &\quad \left. + \lambda \begin{pmatrix} Z'^t \\ L'^t \end{pmatrix} (Z', L') \right)^{-1} \begin{pmatrix} B'^t \\ K'^t \end{pmatrix}, \end{aligned} \quad (31b)$$

$$\begin{aligned} P(\lambda) &= (B', K') \left(\begin{pmatrix} B'^t \\ K'^t \end{pmatrix} (B', K') \right. \\ &\quad \left. + \lambda \begin{pmatrix} Z'^t \\ L'^t \end{pmatrix} (Z', L') \right)^{-1} \begin{pmatrix} B'^t \\ K'^t \end{pmatrix}. \end{aligned} \quad (31c)$$

In eqs. (29)–(31) all the elements of the $n_l \times m$ matrix Z' , the $n_s \times m$ matrix Z_f and the $m \times n_s$ matrix Z_a are zero. I_f is a $n_s \times n_s$ and I_a a $m \times m$ identity matrix.

In order to calculate the result for the problem in section 2, the matrices $K'^{-1}(\lambda)$, $B'^{-1}(\lambda)$ and

$P(\lambda)$ must be evaluated. For that purpose a fast and efficient method is proposed in the following text. This method can be divided into three steps. By performing the first two steps the matrices $K'^{-1}(\lambda)$, $B'^{-1}(\lambda)$ and $P(\lambda)$ can be evaluated for a given value of the regularization parameter. Carrying out the third step a generalized singular value decomposition [24] is obtained and the matrices $K'^{-1}(\lambda)$, $B'^{-1}(\lambda)$ and $P(\lambda)$ can be evaluated for different values of the regularization parameter without further matrix decompositions. As a consequence the time for the calculation of the regularization parameter reduces to such a limit that the calculations can be performed on a simple personal computer.

In the first step the QR-decomposition [25] of the matrix $(s_B B', K')$ is used to reduce the number n of data points in the case of $n > m + n_s$:

$$(s_B B', K') = Q(B'', K''). \quad (32)$$

In this equation the scaling factor s_B given by

$$s_B = \frac{\|K'\|_\infty}{\|B'\|_\infty} \quad (33)$$

is introduced in order to stabilize the decomposition. Q is a $n \times (m + n_s)$ matrix satisfying

$$Q^t Q = I, \quad (34)$$

and (B'', K'') is an upper triangular matrix, composed of the $(m + n_s) \times m$ matrix B'' and the $(m + n_s) \times n_s$ matrix K'' . With these quantities eq. (31) can be written as

$$\begin{aligned} K'^{-1}(\lambda) &= (Z_f, I_f) \left(\begin{pmatrix} B''^t \\ K''^t \end{pmatrix} (B'', K'') \right. \\ &\quad \left. + \lambda \begin{pmatrix} Z'^t \\ L'^t \end{pmatrix} (Z', L') \right)^{-1} \begin{pmatrix} B''^t \\ K''^t \end{pmatrix} Q^t, \end{aligned} \quad (35a)$$

$$\begin{aligned} B'^{-1}(\lambda) &= s_B (I_a, Z_a) \left(\begin{pmatrix} B''^t \\ K''^t \end{pmatrix} (B'', K'') \right. \\ &\quad \left. + \lambda \begin{pmatrix} Z'^t \\ L'^t \end{pmatrix} (Z', L') \right)^{-1} \begin{pmatrix} B''^t \\ K''^t \end{pmatrix} Q^t, \end{aligned} \quad (35b)$$

$$\mathbf{P}(\lambda) = \mathbf{Q}(\mathbf{B}'', \mathbf{K}'') \left(\begin{pmatrix} \mathbf{B}''^t \\ \mathbf{K}''^t \end{pmatrix} (\mathbf{B}'', \mathbf{K}'') + \lambda \begin{pmatrix} \mathbf{Z}'^t \\ \mathbf{L}'^t \end{pmatrix} (\mathbf{Z}', \mathbf{L}') \right)^{-1} \begin{pmatrix} \mathbf{B}''^t \\ \mathbf{K}''^t \end{pmatrix} \mathbf{Q}^t. \quad (35c)$$

In the case of $n \leq (m + n_s)$ the eq. (35) with

$$\mathbf{Q} = \mathbf{I}, \quad (36a)$$

$$\mathbf{K}'' = \mathbf{K}', \quad (36b)$$

$$\mathbf{B}'' = s_B \mathbf{B}' \quad (36c)$$

are also valid.

In fact this first matrix decomposition is not absolutely necessary and the expression for the matrices $\mathbf{K}'^{-1}(\lambda)$, $\mathbf{B}'^{-1}(\lambda)$ and $\mathbf{P}(\lambda)$ can be evaluated omitting this first step. On the other hand time and memory needed for the calculations is reduced by this decomposition, because for $n > (m + n_s)$ the following matrix decompositions are independent of the number n of data points.

In the next step the QR-decomposition of the matrix

$$\begin{pmatrix} (\mathbf{B}'', \mathbf{K}'') \\ s_l(\mathbf{Z}', \mathbf{L}') \end{pmatrix} = \begin{pmatrix} \mathbf{Q}_1 \\ \mathbf{Q}_2 \end{pmatrix} \mathbf{R} \quad (37)$$

is introduced. In this equation s_l is another scaling factor given by

$$s_l = \frac{\|\mathbf{K}'\|_\infty}{\|\mathbf{L}'\|_\infty} \quad (38a)$$

or by

$$s_l = \sqrt{\lambda_0}, \quad (38b)$$

if an appropriate value λ_0 for the regularization parameter λ is known (see also section 4.3). \mathbf{R} is an upper triangular $(m + n_s) \times (m + n_s)$ matrix \mathbf{Q}_1 is a $\min(n, m + n_s) \times (m + n_s)$ matrix and \mathbf{Q}_2 is a $n_l \times (m + n_s)$ matrix. Furthermore, \mathbf{Q}_1 and \mathbf{Q}_2 satisfy the relation

$$\mathbf{Q}_1^t \mathbf{Q}_1 + \mathbf{Q}_2^t \mathbf{Q}_2 = \mathbf{I}. \quad (39)$$

With this decomposition the matrices $\mathbf{K}'^{-1}(\lambda)$, $\mathbf{B}'^{-1}(\lambda)$ and $\mathbf{P}(\lambda)$ can be calculated by

$$\begin{aligned} \mathbf{K}'^{-1}(\lambda) &= (\mathbf{Z}_f, \mathbf{I}_f) \mathbf{R}^{-1} \\ &\times \left(\left(1 - \frac{\lambda}{s_l^2} \right) \mathbf{Q}_1^t \mathbf{Q}_1 + \frac{\lambda}{s_l^2} \mathbf{I} \right)^{-1} \mathbf{Q}_1^t \mathbf{Q}^t, \end{aligned} \quad (40a)$$

$$\begin{aligned} \mathbf{B}'^{-1}(\lambda) &= s_B (\mathbf{I}_a, \mathbf{Z}_a) \mathbf{R}^{-1} \\ &\times \left(\left(1 - \frac{\lambda}{s_l^2} \right) \mathbf{Q}_1^t \mathbf{Q}_1 + \frac{\lambda}{s_l^2} \mathbf{I} \right)^{-1} \mathbf{Q}_1^t \mathbf{Q}^t, \end{aligned} \quad (40b)$$

$$\mathbf{P}(\lambda) = \mathbf{Q} \mathbf{Q}_1 \left(\left(1 - \frac{\lambda}{s_l^2} \right) \mathbf{Q}_1^t \mathbf{Q}_1 + \frac{\lambda}{s_l^2} \mathbf{I} \right)^{-1} \mathbf{Q}_1^t \mathbf{Q}^t. \quad (40c)$$

If the scaling factor s_l is given by eq. (38b), the result can be calculated for the regularization parameter λ_0 :

$$f_\lambda^\sigma = (\mathbf{Z}_f, \mathbf{I}_f) \mathbf{R}^{-1} \mathbf{Q}_1^t \mathbf{Q}^t g'^\sigma, \quad (41a)$$

$$a^\sigma = s_B (\mathbf{I}_a, \mathbf{Z}_a) \mathbf{R}^{-1} \mathbf{Q}_1^t \mathbf{Q}^t g'^\sigma, \quad (41b)$$

$$\begin{aligned} \sigma^2(f_{\lambda i}^\sigma) &= \sigma^2 \left((\mathbf{Z}_f, \mathbf{I}_f) \mathbf{R}^{-1} \mathbf{Q}_1^t \mathbf{Q}_1 (\mathbf{R}^{-1})^t \begin{pmatrix} \mathbf{Z}_f^t \\ \mathbf{I}_f^t \end{pmatrix} \right)_{ii}, \\ i &= 1, \dots, n_s, \end{aligned} \quad (41c)$$

$$\begin{aligned} \sigma^2(a_i^\sigma) &= s_B^2 \sigma^2 \left((\mathbf{I}_a, \mathbf{Z}_a) \mathbf{R}^{-1} \mathbf{Q}_1^t \mathbf{Q}_1 (\mathbf{R}^{-1})^t \begin{pmatrix} \mathbf{I}_a^t \\ \mathbf{Z}_a^t \end{pmatrix} \right)_{ii}, \\ i &= 1, \dots, m. \end{aligned} \quad (41d)$$

Otherwise, if the regularization parameter must be determined with the SC-method, a third step is necessary. In this step the SV-decomposition [1] of \mathbf{Q}_1 is introduced:

$$\mathbf{Q}_1 = \mathbf{U} \mathbf{W} \mathbf{V}^t. \quad (42)$$

Here, \mathbf{U} is a $\min(n, m + n_s) \times \min(n, m + n_s)$ matrix satisfying

$$\mathbf{U}^t \mathbf{U} = \mathbf{I}, \quad (43a)$$

and \mathbf{V} is a $(m + n_s) \times \min(n, m + n_s)$ matrix satisfying

$$\mathbf{V}^t \mathbf{V} = \mathbf{I}. \quad (43b)$$

The matrix \mathbf{W} is a diagonal matrix containing the singular values of \mathbf{Q}_1 . Replacing \mathbf{Q}_1 by $\mathbf{U} \mathbf{W} \mathbf{V}^t$ in eq. (40), the final expressions for the matrices $\mathbf{K}'^{-1}(\lambda)$, $\mathbf{B}'^{-1}(\lambda)$ and $\mathbf{P}(\lambda)$ are obtained:

$$\mathbf{K}'^{-1}(\lambda) = (\mathbf{Z}_f, \mathbf{I}_f) \mathbf{R}^{-1} \mathbf{V} \mathbf{W}^{-1}(\lambda) \mathbf{U}^t \mathbf{Q}^t, \quad (44a)$$

$$\mathbf{B}'^{-1}(\lambda) = s_B (\mathbf{I}_a, \mathbf{Z}_a) \mathbf{R}^{-1} \mathbf{V} \mathbf{W}^{-1}(\lambda) \mathbf{U}^t \mathbf{Q}^t, \quad (44b)$$

$$\mathbf{P}(\lambda) = \mathbf{Q} \mathbf{U} \mathbf{W} \mathbf{W}^{-1}(\lambda) \mathbf{U}^t \mathbf{Q}^t, \quad (44c)$$

with

$$W_{ij}^{-1}(\lambda) = \delta_{ij} \frac{W_{ii}}{(1 - \lambda/s_i^2)W_{ii}^2 + \lambda/s_i^2},$$

$$i, j = 1, \dots, \min(n, m + n_s). \quad (45)$$

Before the result can now be determined, the value λ_{SC} for the regularization parameter λ must be calculated by solving eq. (13) or eq. (18). The quantities needed for this purpose can be obtained with help of the eqs. (9), (14), (19), (20), (22c) and (44):

$$\begin{aligned} ED_f(f_\lambda^\sigma, \mu, \sigma) \\ = h_s \|(\mathbf{Z}_f, \mathbf{I}_f) \mathbf{R}^{-1} \mathbf{V} (\mathbf{I} - \mathbf{W}^{-1}(\mu) \mathbf{W}) \mathbf{W}^{-1}(\lambda) \\ \times \mathbf{U}^t \mathbf{Q}^t \mathbf{g}'^\sigma \|^2 \\ + h_s \sigma^2 \text{trace} \left((\mathbf{Z}_f, \mathbf{I}_f) \mathbf{R}^{-1} \mathbf{V} \mathbf{W}^{-1}(\mu) \right. \\ \left. \times ((\mathbf{Z}_f, \mathbf{I}_f) \mathbf{R}^{-1} \mathbf{V} \mathbf{W}^{-1}(\mu))^t \right) \end{aligned} \quad (46a)$$

$$\begin{aligned} ED_g(f_\lambda^\sigma, \lambda, \sigma) \\ = \|(\mathbf{I} - \mathbf{W} \mathbf{W}^{-1}(\lambda)) \mathbf{W} \mathbf{W}^{-1}(\lambda) \mathbf{U}^t \mathbf{Q}^t \mathbf{g}'^\sigma \|^2 \\ + \sigma^2 \text{trace} \left((\mathbf{I} - \mathbf{W} \mathbf{W}^{-1}(\lambda)) (\mathbf{I} - \mathbf{W} \mathbf{W}^{-1}(\lambda))^t \right) \\ + \sigma^2 \max(0, n - m + n_s) \end{aligned} \quad (46b)$$

$$\begin{aligned} d_g = \|\mathbf{g}'^\sigma\|^2 - \|\mathbf{U}^t \mathbf{Q}^t \mathbf{g}'^\sigma\|^2 \\ + \|(\mathbf{I} - \mathbf{W} \mathbf{W}^{-1}(\lambda)) \mathbf{U}^t \mathbf{Q}^t \mathbf{g}'^\sigma\|^2. \end{aligned} \quad (46c)$$

Then the solution itself can be determined together with the corresponding errors. Because of the eqs. (8), (21) and (44) these quantities are given by

$$f_\lambda^\sigma = (\mathbf{Z}_f, \mathbf{I}_f) \mathbf{R}^{-1} \mathbf{V} \mathbf{W}^{-1}(\lambda_{SC}) \mathbf{U}^t \mathbf{Q}^t \mathbf{g}'^\sigma, \quad (47a)$$

$$\mathbf{a}^\sigma = s_B(\mathbf{I}_a, \mathbf{Z}_a) \mathbf{R}^{-1} \mathbf{V} \mathbf{W}^{-1}(\lambda_{SC}) \mathbf{U}^t \mathbf{Q}^t \mathbf{g}'^\sigma, \quad (47b)$$

$$\begin{aligned} \sigma^2(f_{\lambda i}^\sigma) = \sigma^2 \left((\mathbf{Z}_f, \mathbf{I}_f) \mathbf{R}^{-1} \mathbf{V} \mathbf{W}^{-1}(\lambda_{SC}) \right. \\ \left. \times ((\mathbf{Z}_f, \mathbf{I}_f) \mathbf{R}^{-1} \mathbf{V} \mathbf{W}^{-1}(\lambda_{SC}))^t \right)_{ii}, \end{aligned} \quad (47c)$$

$$\begin{aligned} \sigma^2(a_i^\sigma) = s_B^2 \sigma^2 \left((\mathbf{I}_a, \mathbf{Z}_a) \mathbf{R}^{-1} \mathbf{V} \mathbf{W}^{-1}(\lambda_{SC}) \right. \\ \left. \times ((\mathbf{I}_a, \mathbf{Z}_a) \mathbf{R}^{-1} \mathbf{V} \mathbf{W}^{-1}(\lambda_{SC}))^t \right)_{ii}. \end{aligned} \quad (47d)$$

Finally, the various steps necessary to compute the result are summarized. If an appropriate value λ_0 for the regularization parameter is known, the calculation can be performed in 6 steps:

1. initialize $n, m, n_s, n_l, \mathbf{B}', \mathbf{K}', \mathbf{L}', \sigma$ and λ_0 ;
2. set s_B (eq. (33));
3. $n \leq m + n_s$: set $\mathbf{K}'' = \mathbf{K}', \mathbf{B}'' = s_B \mathbf{B}'$ and $(\mathbf{Q}^t \mathbf{g}'^\sigma) = \mathbf{g}'^\sigma$;
 $n > m + n_s$: determine $\mathbf{K}'', \mathbf{B}''$ and $(\mathbf{Q}^t \mathbf{g}'^\sigma)$ by QR-decomposition (eq. (32));
4. set s_l (eq. (38b)) and determine \mathbf{Q}_l and \mathbf{R} by QR-decomposition (eq. (37));
5. calculate $(\mathbf{R}^{-1} \mathbf{Q}_l^t)$;
6. calculate $f_\lambda^\sigma, \mathbf{a}^\sigma, \sigma(f_{\lambda i}^\sigma)$ and $\sigma(a_i^\sigma)$ (eq. (41)).

If an appropriate value for the regularization parameter is not known, the first 4 steps remain nearly the same. Then additional steps are necessary for the determination of the regularization parameter:

1. initialize $n, m, n_s, n_l, \mathbf{B}', \mathbf{K}', \mathbf{L}'$ and σ , if known;
2. set s_B (eq. (33));
3. $n \leq m + n_s$: set $\mathbf{K}'' = \mathbf{K}', \mathbf{B}'' = s_B \mathbf{B}'$ and $(\mathbf{Q}^t \mathbf{g}'^\sigma) = \mathbf{g}'^\sigma$;
 $n > m + n_s$: determine $\mathbf{K}'', \mathbf{B}''$ and $(\mathbf{Q}^t \mathbf{g}'^\sigma)$ by QR-decomposition (eq. (32));
4. set s_l (eq. (38a)) and determine \mathbf{Q}_l and \mathbf{R} by QR-decomposition (eq. (37));
5. determine \mathbf{V}, \mathbf{W} and $(\mathbf{U}^t \mathbf{Q}^t \mathbf{g}'^\sigma)$ by SV-decomposition (eq. (42));
6. calculate $(\mathbf{R}^{-1} \mathbf{V})$;
7. determine λ_{SC} by solving eq. (13) or eq. (18), if an estimate for the scaling factor σ must be calculated;
8. calculate $f_\lambda^\sigma, \mathbf{a}^\sigma, \sigma(f_{\lambda i}^\sigma)$ and $\sigma(a_i^\sigma)$ (eq. (47)).

4.3. Calculation of the result with constraints

In the case of additional constraints the same QR-decomposition as described in section 4.2 (eqs. (32)–(36)) is used to reduce the number n of data points. With the quantities introduced there the result is obtained by minimizing

$$\begin{aligned} V(\lambda) = \|\mathbf{Q}^t \mathbf{g}'^\sigma - (\mathbf{K}'' \mathbf{f} + s_B^{-1} \mathbf{B}'' \mathbf{a})\|^2 + \lambda \|\mathbf{L}' \mathbf{f}\|^2 \\ + \|\mathbf{g}'^\sigma\|^2 - \|\mathbf{Q}^t \mathbf{g}'^\sigma\|^2 \end{aligned} \quad (48)$$

subject to the constraints

$$f_i \geq 0, \quad i = 1, \dots, n_s. \quad (49)$$

If an appropriate value for the regularization parameter λ is not known, it can be determined with the SC-method. However, it is convenient to apply the SC-method in a modified way, because the quantities $ED_f(f, \lambda, \sigma)$ and $ED_g(f, \lambda, \sigma)$ can not be calculated explicitly, if the constraints (49) must be considered.

Using the modified SC-method, the determination of the regularization parameter is composed of three steps. In the first step a value λ'_{SC} for the regularization parameter λ and, if necessary, an estimate $\hat{\sigma}$ for the scaling factor σ is calculated neglecting the constraints (49). In the second step, an intermediate result is determined by minimizing $V(\lambda'_{SC})$ subject to the constraints (49). This minimization can be done by a QP-algorithm [26] and leads to a set \mathcal{M}' of active constraints:

$$f_{\lambda i}^\sigma = 0, \quad i \in \mathcal{M}'. \quad (50)$$

In the third step the final value λ_{SC} for the regularization parameter λ is determined. For this purpose again the SC-method is used. But this time the set \mathcal{M}' of active constraints is taken into account by removing the columns from the matrices \mathbf{K}'' and \mathbf{L}' which belong to an active constraint.

If a value for the regularization parameter is given or has been calculated with the modified SC-method, the final result is obtained by minimizing $V(\lambda_0)$ or $V(\lambda_{SC})$ subject to the constraints (49). By doing this, the set \mathcal{M} of active constraints for the final result is obtained. This set is used for the determination of the error intervals, because an explicit expression for these intervals can not be obtained, if the constraints (49) are considered. For this purpose the columns of the matrices \mathbf{K}'' and \mathbf{L}' which belong to an active constraint are removed. Using the modified matrices, the error intervals can then be calculated as described in section 4.2 (see eqs. (37) and (41)).

Again, the steps necessary to calculate the

result are summarized. If a value λ_0 for the regularization parameter λ is given, the computation can be divided into 8 steps:

1. initialize $n, m, n_s, n_l, \mathbf{B}', \mathbf{K}', \mathbf{L}', \sigma$ and λ_0 ;
 2. set s_B (eq. (33));
 3. $n \leq m + n_s$: set $\mathbf{K}'' = \mathbf{K}', \mathbf{B}'' = s_B \mathbf{B}'$ and $(\mathbf{Q}' \mathbf{g}'^\sigma) = \mathbf{g}'^\sigma$;
 $n > m + n_s$: determine $\mathbf{K}'', \mathbf{B}''$ and $(\mathbf{Q}' \mathbf{g}'^\sigma)$ by QR-decomposition (eq. (32));
 4. determine $f_{\lambda i}^\sigma, a_i^\sigma$ and the set \mathcal{M} of active constraints by minimizing $V(\lambda_0)$ subject to the constraints (49);
 5. determine \mathbf{K}_m'' and \mathbf{L}_m' by removing the columns from \mathbf{K}'' and \mathbf{L}' which belong to an active constraint;
 6. set s_l (eq. (38b)) and determine \mathbf{Q}_1 and \mathbf{R} by QR-decomposition (eq. (37) with \mathbf{K}'' and \mathbf{L}' replaced by \mathbf{K}_m'' and \mathbf{L}_m');
 7. calculate $(\mathbf{R}^{-1} \mathbf{Q}_1^t)$;
 8. calculate $\sigma(f_{\lambda i}^\sigma)$ for $i \notin \mathcal{M}$ and $\sigma(a_i^\sigma)$ (eq. (41)).
- If in addition a value for the regularization parameter must be determined, several additional steps are necessary:

1. initialize $n, m, n_s, n_l, \mathbf{B}', \mathbf{K}', \mathbf{L}'$ and σ , if known;
2. set s_B (eq. (33));
3. $n \leq m + n_s$: set $\mathbf{K}'' = \mathbf{K}', \mathbf{B}'' = s_B \mathbf{B}'$ and $(\mathbf{Q}' \mathbf{g}'^\sigma) = \mathbf{g}'^\sigma$;
 $n > m + n_s$: determine $\mathbf{K}'', \mathbf{B}''$ and $(\mathbf{Q}' \mathbf{g}'^\sigma)$ by QR-decomposition (eq. (32));
4. set s_l (eq. (38a)) and determine \mathbf{Q}_1 and \mathbf{R} by QR-decomposition (eq. (37));
5. determine \mathbf{V}, \mathbf{W} and $(\mathbf{U}^t \mathbf{Q}' \mathbf{g}'^\sigma)$ by SV-decomposition (eq. (42));
6. calculate $(\mathbf{R}^{-1} \mathbf{V})$;
7. determine the preliminary value λ'_{SC} for the regularization parameter λ by solving eq. (13) or eq. (18), if in addition an estimate for the scaling factor σ must be calculated;
8. determine the set \mathcal{M}' of active constraints by minimizing $V(\lambda'_{SC})$ subject to the constraints (49);
9. determine \mathbf{K}_m'' and \mathbf{L}_m' by removing the columns from \mathbf{K}'' and \mathbf{L}' which belong to an active constraint;
10. set s_l (eq. (38a)) and determine \mathbf{Q}_1 and \mathbf{R} by QR-decomposition (eq. (37) with \mathbf{K}'' and \mathbf{L}' replaced by \mathbf{K}_m'' and \mathbf{L}_m');

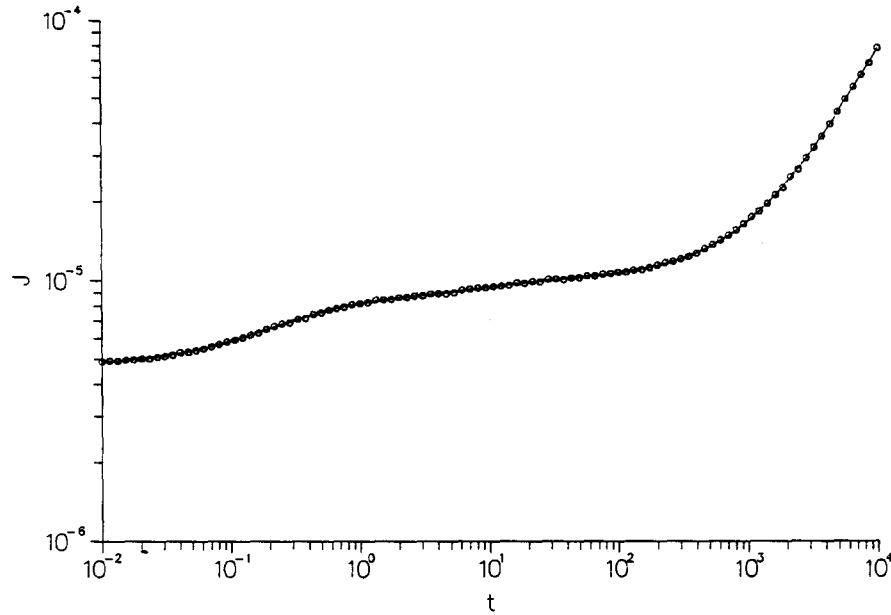


Fig. 1. Creep compliance J . The solid line shows the values calculated from the original spectrum (fig. 2) with J_e and $1/\eta_0$ given by table 1. The simulated data are marked by circles.

11. determine \mathbf{V} , \mathbf{W} and $(\mathbf{U}^t \mathbf{Q}^t g'^\sigma)$ by SV-decomposition (eq. (42));
12. calculate $(\mathbf{R}^{-1} \mathbf{V})$;

13. determine the final value λ_{SC} for the regularization parameter λ by solving eq. (13);
14. determine f_λ^σ , a^σ and the set \mathcal{M} of active

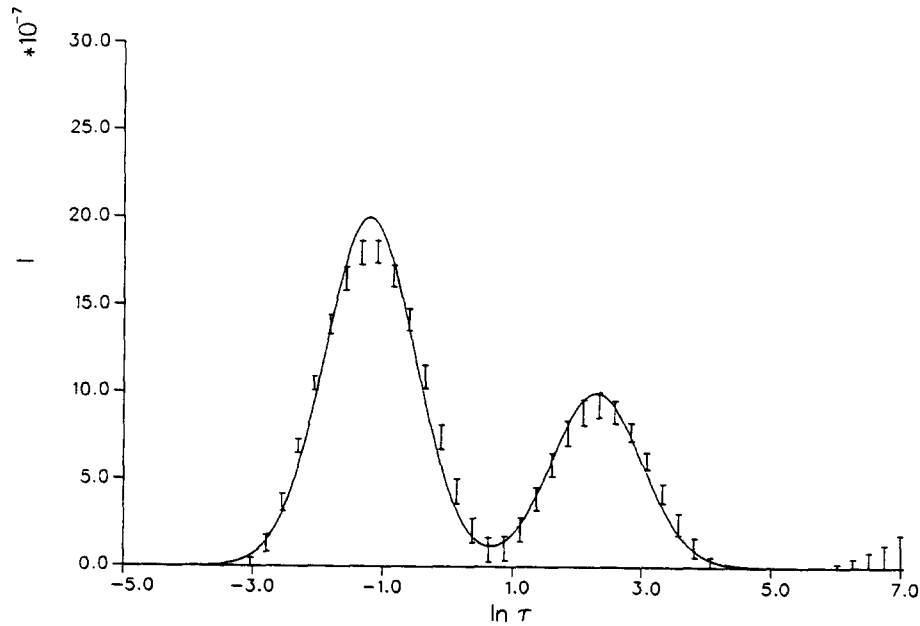


Fig. 2. Retardation spectrum l . The solid line shows the original spectrum. The spectrum obtained by the solution method from the simulated data is marked by the error intervals.

- constrains by minimizing $V(\lambda_{SC})$ subject to the constraints (49);
15. determine \mathbf{K}_m'' and \mathbf{L}_m' by removing the columns from \mathbf{K}'' and \mathbf{L}' which belong to an active constraint;
 16. set $s_l = \sqrt{\lambda_{SC}}$ and determine \mathbf{Q}_1 and \mathbf{R} by QR-decomposition (eq. (37) with \mathbf{K}'' and \mathbf{L}' replaced by \mathbf{K}_m'' and \mathbf{L}_m');
 17. calculate $(\mathbf{R}^{-1}\mathbf{Q}_1^t)$;
 18. calculate $\sigma(f_{\lambda_i}^\sigma)$ for $i \notin \mathcal{M}$ and $\sigma(a_i^\sigma)$ (eq. (41)).

5. An example for the application of the solution method

In this section the most important features of the solution method are illustrated. For that purpose the solution method is applied to simulated data. As an example the determination of the retardation spectrum l defined in the linear theory of viscoelastic fluids [27] is used. This spectrum is related to the creep compliance J , the equilibrium compliance J_e and the steady-state viscosity (at vanishing shear rate) η_0 by

$$J(t) = J_e - \int_{-\infty}^{+\infty} e^{-t/\tau} l(\ln \tau) d \ln \tau + t/\eta_0. \quad (51)$$

In order to generate simulated data for the creep compliance J a retardation spectrum l (fig. 2) and values for the equilibrium compliance J_e and the reciprocal of the steady-state viscosity η_0 (table 1) have been chosen which could represent the linear viscoelastic properties of a polymer melt in the terminal region. Using this spectrum

and the values for J_e and $1/\eta_0$, the corresponding creep compliance J was calculated according to eq. (51). Finally, the simulated data $J_1^\sigma, \dots, J_{100}^\sigma$ (fig. 1) were obtained by adding a relative error of 0.5% to the creep compliance J at the discrete points $t = t_i$.

With

$$g(t) = J(t), \quad (52a)$$

$$s = \ln \tau, \quad (52b)$$

$$f(s) = l(\ln \tau), \quad (52c)$$

$$a_1 = J_e, \quad (52d)$$

$$a_2 = 1/\eta_0, \quad (52e)$$

$$K(t, s) = -e^{-te^{-s}}, \quad (52f)$$

$$b_1(t) = 1, \quad (52g)$$

$$b_2(t) = t, \quad (52h)$$

$$g_i^\sigma = J_i^\sigma, \quad i = 1, \dots, 100, \quad (52i)$$

$$\sigma_i = J_i^\sigma, \quad i = 1, \dots, 100, \quad (52j)$$

the determination of the retardation spectrum l given the values $J_1^\sigma, \dots, J_{100}^\sigma$ is the same problem as in section 2. Therefore, the retardation spectrum l can be calculated as described in section 3 and 4 and the program FTIKREG can be used to perform the calculation. The results obtained with $s_{\min} = -5$, $s_{\max} = 7$, $n_s = 50$ and $\mathbf{L}f = f''$ are shown in fig. 2 and table 1.

First it should be noted, that a good value for the regularization parameter ($\lambda_{SC} = 1.852 \times 10^7$) has been calculated: The values for the retardation spectrum l , the equilibrium compliance J_e and the reciprocal of the steady-state viscosity η_0 agree well with the values used for the simulation of the data. Also the estimate $\hat{\sigma}$ for the relative error is in good agreement with the true value. Finally, it should be noted, that the time needed for the calculation on a 386SX personal computer (20 MHz, 2 MB RAM) is about 50 seconds. Of course this time increases with the number n of data points and the number n_s of points, at which the solution is calculated. But usually a personal computer is sufficient for the solution of such a problem.

Table 1

Values for the equilibrium compliance J_e , the reciprocal of the steady-state viscosity η_0 and the relative error σ . The second column contains the true values used to simulate the data. The third column contains the values obtained by the solution method from the simulated data

	True values	Estimated values
J_e	1.0000×10^{-5}	$1.0050 \times 10^{-5} \pm 0.0062 \times 10^{-5}$
$1/\eta_0$	6.6667×10^{-9}	$6.6526 \times 10^{-9} \pm 0.0213 \times 10^{-9}$
σ	5.0000×10^{-3}	5.1659×10^{-3}

6. Conclusions

A fast and reliable method for the solution of Fredholm integral equations of the first kind given noisy experimental data has been presented together with the computer program FTIKREG. The solution method is based on Tikhonov regularization. For the determination of the regularization parameter the SC-method is used. Also an efficient way for the computation of the solution based on a kind of generalized singular-value decomposition has been proposed. The solution method has been tested using simulated data and led to good results. As an example the determination of the retardation spectrum defined in the linear theory of viscoelastic fluids was used. This example has also shown that with the program FTIKREG such a problem can be solved on a personal computer within one minute. The program FTIKREG can be obtained together with a user manual from the CPC Program Library.

Acknowledgements

I would like to acknowledge the financial support by Rheometrics Inc., New Jersey. I thank Prof. A. Neumaier for the hint at generalized singular-value decompositions and Prof. J. Honerkamp and D. Grabowski for stimulating discussion and the help in preparing the manuscript.

References

- [1] W.H. Press, B.P. Flannery, S.A. Teukolsky and W.T. Vetterling, *Numerical Recipes* (Cambridge Univ. Press, Cambridge, 1986).
- [2] V.A. Morozov, *Methods for Solving Incorrectly Posed Problems* (Springer, Berlin, 1984).
- [3] C.T.H. Baker, *The Numerical Treatment of Integral Equations* (Clarendon, Oxford, 1974).
- [4] M. Bertero, in: *Inverse Problems*, G. Talenti, ed. (Springer, Berlin, 1986).
- [5] L.M. Delves and J. Walsh, *The Numerical Treatment of Integral Equations* (Clarendon, Oxford, 1974).
- [6] B.R. Frieden, in: *Picture Processing and Digital Filtering*, T.S. Huang, ed. (Springer, Berlin, 1979).
- [7] A.K. Louis, *Inverse und schlecht gestellte Probleme* (Teubner, Stuttgart, 1989).
- [8] C.W. Groetsch, *The Theory of Tikhonov Regularization for Fredholm Equations of the First Kind* (Pitman, London, 1984).
- [9] S.W. Provencher, *Comput. Phys. Commun.* 27 (1982) 213.
- [10] S.W. Provencher, *Comput. Phys. Commun.* 27 (1982) 229.
- [11] W. Brown, R. Johnson, P. Štěpánek and P. Jakeš, *Macromolecules* 21 (1988) 2859.
- [12] G. Vansco, I. Tomka and K. Vansco-Polacsek, *Macromolecules* 21 (1988) 415.
- [13] S.F. Gull and J. Skilling, *IEE Proc. F* 131 (1984) 646.
- [14] P. Craven and G. Whaba, *Numer. Math.* 31 (1979) 377.
- [15] A.R. Davies and R.S. Anderssen, *J. Austral. Math. Soc. B* 28 (1986) 114.
- [16] H.W. Engl and H. Gfrerer, *Appl. Numer. Math.* 4 (1988) 395.
- [17] H.W. Engl and A. Neubauer, in: *Constructive Methods for the Practical Treatment of Integral Equations*, G. Hämmerlin and K.H. Hoffmann, eds. (Birkhäuser, Basel, 1985).
- [18] H. Gfrerer, *Math. Comput.* 49 (1987) 507.
- [19] C.W. Groetsch, in: *Improperly Posed Problems and their Numerical Treatment*, G. Hämmerlin and K.H. Hoffmann, eds. (Birkhäuser, Basel, 1983).
- [20] J.T. King and A. Neubauer, *Computing* 40 (1988) 91.
- [21] G. Whaba, in: *Solution Methods for Integral Equations*, M.A. Golberg, ed. (Plenum, New York, 1978).
- [22] J. Honerkamp and J. Weese, *Continuum Mech. Thermodyn.* 2 (1990) 17.
- [23] J. Weese, *Diploma thesis, Universität Freiburg* (1989).
- [24] C. van Loan, *SIAM J. Numer. Anal.* 13 (1976) 76.
- [25] J. Stoer, *Numerische Mathematik 1* (Springer, Berlin, 1989).
- [26] J. Stoer, *SIAM J. Numer. Anal.* 8 (1971) 382.
- [27] J.D. Ferry, *Viscoelastic properties of Polymers* (Wiley, New York, 1980).